AD
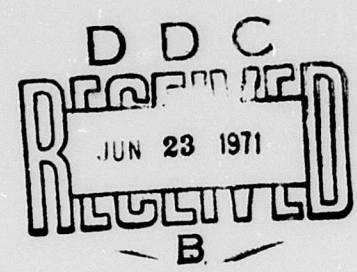
USAAVLABS TECHNICAL REPORT 71-13

INVESTIGATION OF FEASIBILITY OF INTEGRAL GAS TURBINE ENGINE SOLID PARTICLE INLET SEPARATORS

PHASE II, FEASIBILITY DEMONSTRATION

By

William J. McAnally, III
Max T. Schilling

April 1971

D D C
RECEIVED
JUN 23 1971
B

EUSTIS DIRECTORATE

U. S. ARMY AIR MOBILITY RESEARCH AND DEVELOPMENT LABORATORY

FORT EUSTIS, VIRGINIA

U S ARMY
MATERIEL COMMAND

Approved for public release;
distribution unlimited.

65

DISCLAIMERS

DOCUMENT CONTROL DATA - R & D

(Security classification of title, body of abstract and indexing annotation must be entered when the overall report is classified)

1. ORIGINATING ACTIVITY (Corporate author)	2a. REPORT SECURITY CLASSIFICATION
Pratt & Whitney Aircraft Division of United Aircraft Corp., Florida Research & Development Center West Palm Beach, Florida	Unclassified
	2b. GROUP

3. REPORT TITLE

INVESTIGATION OF FEASIBILITY OF INTEGRAL GAS TURBINE ENGINE SOLID PARTICLE INLET SEPARATORS

4. DESCRIPTIVE NOTES *(Type of report and inclusive dates)*

Final Report, Phase II, Feasibility Demonstration

5. AUTHOR(S) *(First name, middle initial, last name)*

W. J. McAnally, III
M. T. Schilling

6. REPORT DATE	7a. TOTAL NO. OF PAGES	7b. NO. OF REFS
April 1971	63	2

8a. CONTRACT OR GRANT NO.	9a. ORIGINATOR'S REPORT NUMBER(S)
DAAJ02-70-C-0003	
b. PROJECT NO.	USAAVLABS Technical Report 71-13
c. Task 1G162207AA7104	9b. OTHER REPORT NO(S) (Any other numbers that may be assigned this report)
d.	PWA FR-4197

10. DISTRIBUTION STATEMENT

Approved for public release; distribution unlimited.

11. SUPPLEMENTARY NOTES	12. SPONSORING MILITARY ACTIVITY
	Eustis Directorate U.S. Army Air Mobility R&D Laboratory Fort Eustis, Virginia

13. ABSTRACT

Helicopter operations for unimproved landing sites have demonstrated the vulnerability of unprotected gas turbine engines to sand and dust ingestion. As an interim solution, engine inlet filtration or particle separator devices have been added to engines and aircraft that were already designed and developed. However, there is a need for particle separators designed to be integral with the engine from its conception to minimize penalties in engine performance, weight, maintainability, and reliability. The objective of this program was to conduct a two-phase investigation of particle separators intended to be an integral part of future advanced-technology gas turbine engines.

In Phase I, eight separator concepts were evaluated with respect to each other, and the two most promising concepts, "semi-reverse-flow" and "powered-mixed-flow," were selected for feasibility demonstration. The effort reported herein describes the work accomplished during Phase II, two different sand and dust particle separator test rigs were fabricated and tested to evaluate separation efficiency, aerodynamic performance characteristics, and operation in rain and foliage ingestion conditions. The semi-reverse-flow separator utilized fixed turning vanes on a contoured hub to induce swirl in an annular duct. At design airflow of 8 lb/sec and 40% scavenge flow, it demonstrated 88.5% separation efficiency with AC coarse test dust at an average pressure drop of 2.8 in. H_2O. The powered-mixed-flow separator attempted to utilize the strong centrifugal field available in a mixed-flow impeller turning at the high speeds characteristic of small gas turbine engines to achieve particle separation. At the design airflow of 8 lb/sec, it demonstrated a maximum separation efficiency of 58.7% with 8.4% scavenge flow and an average pressure rise of 6.76 psi.

Both separator concepts were determined to be feasible and the semi-reverse-flow separator is considered to be superior to current engine air particle separators for the majority of aspects investigated, but the powered mixed-flow separator was determined to be inferior to current separators. However, neither the semi-reverse-flow separator nor the powered-mixed-flow separator separator should be considered an optimum design. A suitable scavenge system, e.g., engine exhaust-gas ejector, has not been demonstrated for the semi-reverse-flow concept. Additional development of the powered-mixed-flow separator may significantly improve separation efficiency, but impeller wear will still be a problem.

DD FORM 1473 REPLACES DD FORM 1473, 1 JAN 64, WHICH IS OBSOLETE FOR ARMY USE.

14. KEY WORDS	LINK A		LINK B		LINK C	
	ROLE	WT	ROLE	WT	ROLE	WT
Particle Separator Investigation						
Integral Engine Inlet Separators						
Experimental Separator Performance						
Semi-Reverse-Flow Separator						
Powered Mixed-Flow Separator						

DEPARTMENT OF THE ARMY
U. S. ARMY AIR MOBILITY RESEARCH & DEVELOPMENT LABORATORY
EUSTIS DIRECTORATE
FORT EUSTIS, VIRGINIA 23604

The objectives of this contractual effort were to demonstrate
the feasibility of two separator concepts selected during
Phase I of the work to function as integral parts of aircraft
gas turbine engines, and to test the two concepts' dust
separation efficiency, effects on engine performance, and
capability for operation in an adverse environment.

This report was prepared by Pratt & Whitney Aircraft Division
of United Aircraft Corporation under the terms of Contract
DAAJ02-70-C-0003. It describes the separator fabrication,
testing, and the results of the tests conducted during Phase II
of the effort.

This report has been reviewed by technical personnel of this
Directorate, and the conclusions contained herein are concurred
in by this Directorate. The U.S. Army Project Engineer for
this effort was Mr. Robert A Langworthy.

INVESTIGATION OF FEASIBILITY OF INTEGRAL GAS TURBINE
ENGINE SOLID PARTICLE INLET SEPARATORS

Final Report

Phase II, Feasibility Demonstration

**Details of illustrations in
this document may be better
studied on microfiche**

By

William J. McAnally, III
Max T. Schilling

Prepared By

Pratt & Whitney Aircraft Division
United Aircraft Corporation
Florida Research and Development Center
West Palm Beach, Florida

for

EUSTIS DIRECTORATE
U. S. ARMY AIR MOBILITY RESEARCH AND DEVELOPMENT LABORATORY
FORT EUSTIS, VIRGINIA

SUMMARY

Helicopter operations from unimproved landing sites have demonstrated the vulnerability of unprotected gas turbine engines to sand and dust ingestion. As an interim solution, engine inlet filtration or particle separator devices have been added to engines and aircraft that were already designed and developed. However, there is a need for particle separators designed to be integral with the engine from its conception to minimize penalties in engine performance, weight, maintainability, and reliability. The objective of this program was to conduct a two-phase investigation of particle separators intended to be an integral part of future advanced-technology gas turbine engines. Phase I involved feasibility study and design; Phase II involved feasibility demonstration.

In Phase I, eight separator concepts were evaluated with respect to each other, and the two most promising concepts, "semi-reverse-flow" and "powered mixed-flow," were selected for feasibility demonstration. The effort reported herein describes the work accomplished during Phase II. Two different sand and dust particle separator test rigs were fabricated and tested to evaluate separation efficiency, aerodynamic performance characteristics, and operation in rain and foliage ingestion conditions. The semi-reverse-flow separator utilized fixed turning vanes on a contoured hub to induce swirl in an annular duct. At design airflow of 8 lb/sec and 40% scavenge flow, the semi-reverse-flow separator demonstrated 88.5% separation efficiency with AC coarse test dust at an average pressure drop of 2.8 in. H_2O. The powered mixed-flow separator attempted to utilize the strong centrifugal field available in a mixed-flow impeller turning at the high speeds characteristic of small gas turbine engines to achieve particle separation. At the design airflow of 8 lb/sec, it demonstrated a maximum separation efficiency of 58.7% with 8.4% scavenge flow and an average pressure rise of 6.76 psi.

In Phase I, both of the selected separator concepts were considered to be potentially superior to current particle separators. Based on the results of the Phase II evaluation, both separator concepts were determined to be feasible and the semi-reverse-flow separator is considered to be superior to current engine air particle separators for the majority of aspects investigated. However, the powered mixed-flow separator was determined to be inferior to current separators. Neither the semi-reverse-flow separator nor the powered-mixed-flow separator should be considered an optimum design. A suitable scavenge system, e.g., engine exhaust-gas ejector, has not been demonstrated for the semi-reverse-flow concept. Additional development of the powered mixed-flow separator may significantly improve separation efficiency, but impeller wear will still be a problem.

TABLE OF CONTENTS

LIST OF ILLUSTRATIONS

LIST OF ILLUSTRATIONS (Continued)

LIST OF ILLUSTRATIONS (Continued)

LIST OF TABLES

LIST OF SYMBOLS

P_{T_0} Bellmouth inlet total pressure, psia or in. H_2O (as indicated)

T_{T_0} Bellmouth inlet total temperature, °R

P_T Total pressure, psia or in. H_2O (as indicated)

T_T Total temperature, °R

W Mass flow, lb_m/sec

β Swirl angle, deg

ΔP Total pressure drop, in. H_2O

δ Impeller inlet total pressure correction factor = $P_T/2116$

η Compressor aerodynamic efficiency

θ Impeller inlet total temperature correction factor = $T_T/519.6$

μ Microns, meters x 10^{-6}

INTRODUCTION

Because gas turbine engines require high airflow per horsepower, they have always been vulnerable to degradation caused by erosive particle contaminants in the air. When subjected to such contamination, degradation is evidenced by loss of power, loss of surge margin, and attendant increased specific fuel consumption due to either erosion or fouling of precision airfoil sections in the compressor and turbine. The majority of early gas-turbine-engine experience was obtained with fixed-wing aircraft operating from paved runways, and particle ingestion was not a significant problem under those conditions. However, recent tactical helicopter operations from unimproved landing sites have forced a reappraisal of the vulnerability of gas turbines to solid-particle ingestion. Figure 1 shows helicopters operating under these adverse conditions. Premature engine removals due to resultant erosion damage have drastically reduced the time between overhaul (TBO), in some cases by a factor of 10 or more. Generally, when the engines were overhauled, all compressor components had to be replaced. As a result, virtually all helicopters now operating in Southeast Asia have some form of protection against sand and dust ingestion.

Two approaches to solving the problem were apparent: either remove the particles from the airstream, or make the engines more erosion resistant. Because the need was urgent and the particle-removal approach was best suited to quick implementation, this was the course adopted by both engine and airframe manufacturers. Particle removal was accomplished by several differing concepts of both barrier filters and inertial devices.

Figure 1. Helicopters Operating From Unimproved Landing Sites.

1

The engine inlet filtration devices now in use have all been developed as "field fixes"; i.e., they were added as an afterthought to an already designed and developed engine and aircraft. There have been few recent improvements in the state of the art of engine inlet protection devices. Basically, most manufacturers have taken filtration concepts used for years in the industrial gas handling field and have modified them to meet the more stringent volume and weight limitations imposed by flight-type hardware. However, both the static-type filters and the inertial separators produced thus far suffer from some serious drawbacks, such as reduced engine performance, increased aircraft weight, maintenance requirements, lack of anti-icing, and FOD problems attributed to the separator itself. At the same time, field tests, as well as new gas turbine developments, are creating increasingly stringent requirements for greater engine protection, higher efficiency, and smaller package size for a given airflow. An engine inlet particle separator that is designed as an integral part of the engine may offer advantages of reduced penalties in engine performance, weight, maintainability, and reliability, as well as make the separator design invariant with aircraft installation. As a result, there is a need to investigate separators designed to be integral with the engine from its conception, to determine if the above penalties can be minimized and if the conflicting requirements of minimum weight and volume, high efficiency, and low pressure drop can be satisfied.

The objective of this program was to conduct an analytical and experimental investigation of the feasibility of particle separators intended to be an integral part of the inlet of future advanced-technology gas turbine engines. The 12-month program was conducted in two phases. Phase I, Feasibility Study and Design, consisted of four tasks: (1) review current separators, (2) determine feasibility of new concepts, (3) select two concepts for testing, and (4) prepare manufacturing drawings. Phase II, Feasibility Demonstration, consisted of two tasks: (1) fabricate two separators, and (2) test two separators.

This report describes the work accomplished during Phase II, Feasibility Demonstration. Phase I effort has already been reported in Reference 1. A maximum airflow rate of 8 lb/sec was chosen as a matter of convenience to facilitate the investigation.

TASK I - FABRICATION OF SEPARATORS

Non-flight-weight test hardware was procured and assembled to evaluate experimentally the semi-reverse-flow and the powered mixed-flow separator concepts that had been selected and approved for feasibility demonstration in Phase I. The rig designed to test the semi-reverse-flow separator concept was entirely new. The rig designed to test the powered mixed-flow separator concept was an adaptation of a rig previously used for conducting a 10-hr sand-ingestion test with a single-stage centrifugal compressor impeller.

Semi-Reverse-Flow Separator Description

The semi-reverse-flow separator, shown schematically in Figure 2, is basically composed of three pieces, all constructed of aluminum. The first sec ion is a flow-measurement, bellmouth-inlet adapter, which connects the rig to the facility dust feeder screen basket assembly. The inlet contains four pitot-static probes, circumferentially spaced between and aft of the four inlet struts (See Figure 3.)

The center piece is the semi-reverse-flow concept test section, designed so that it may be tested with and without swirl vanes. The swirl vanes were stamped of 0.100-in.-thick aluminum and then welded into slots machined in the coanda-ramp hub. A total of 18 swirl vanes, each having a 30-deg nominal swirl angle, were cantilevered from the hub and stacked about the vane chord midpoint. A photograph of the hub with the swirl vanes attached is shown in Figure 4. A second hub was also manufactured, identical in contour, but without swirl vanes, to permit testing of a no-swirl configuration.

The rear section is an adapter, which simulates an 8.0-lb/sec compressor inlet and incorporates a particle-scavenge duct sized for a flow rate equal to 40% of the design primary flow. The annular scavenge collection manifold has two scavenge discharge ports, located 180-deg apart, which provide for flow of the separated dust to the two final filters connected to the B-2/B-33 facility ejector system. The clean primary flow air is discharged through the center of the rig into a facility ejector line. The simulated compressor inlet plane contains a five-position traversing cobra probe, and the scavenge duct contains a midspan fixed-position cobra probe. Both probes measure total pressure and swirl angle. An assembled view of the semi-reverse-flow separator hardware ready for testing is shown in Figure 5.

Powered Mixed-Flow Separator Description

The powered mixed-flow separator hardware, shown schematically in Figure 6, is an adaptation of an existing single-stage compressor rig that was previously used for conducting a sand-ingestion test. The rig basically consists of an inlet section, a mixed-flow impeller with a special bearing system, and separate annular collection chambers for segregating the scavenge-discharge and clean-air flows.
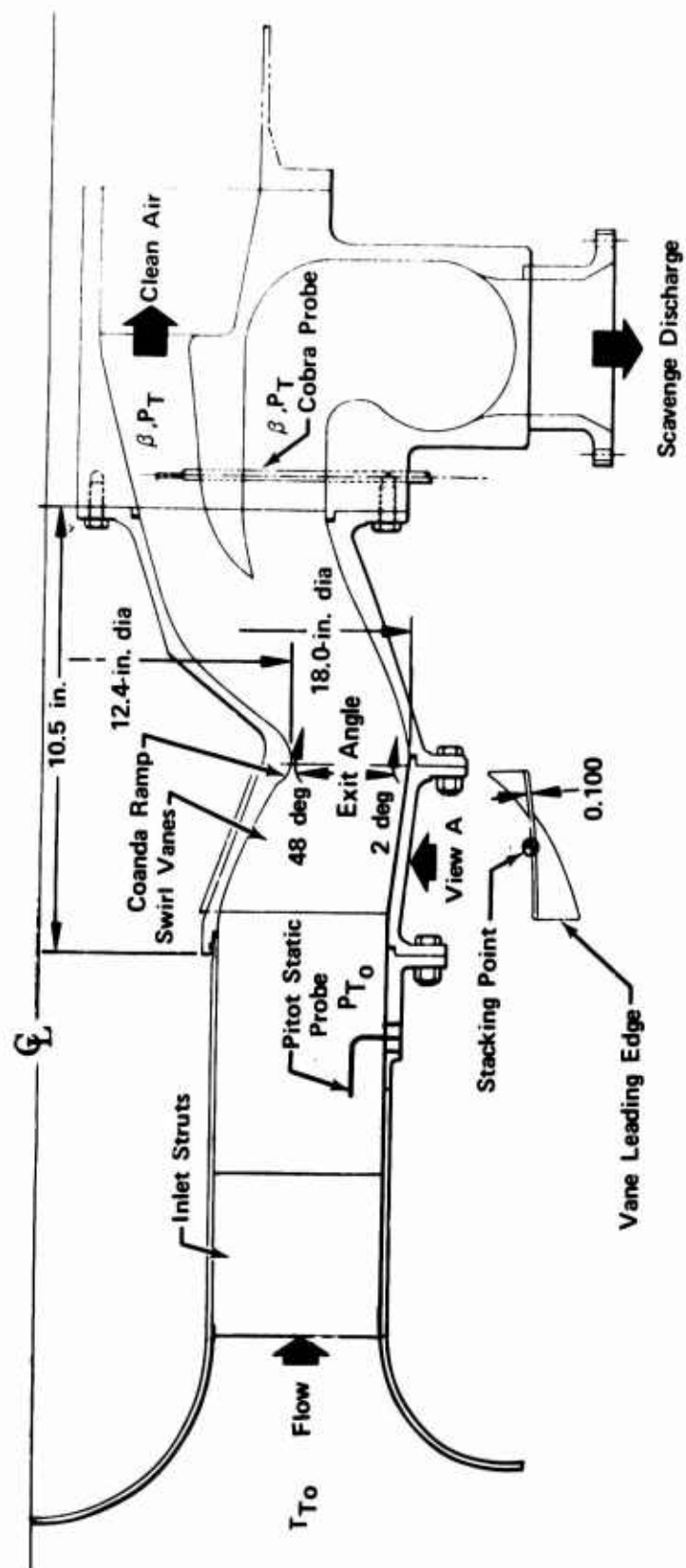
Figure 2. Semi-Reverse-Flow Particle Separator Schematic.
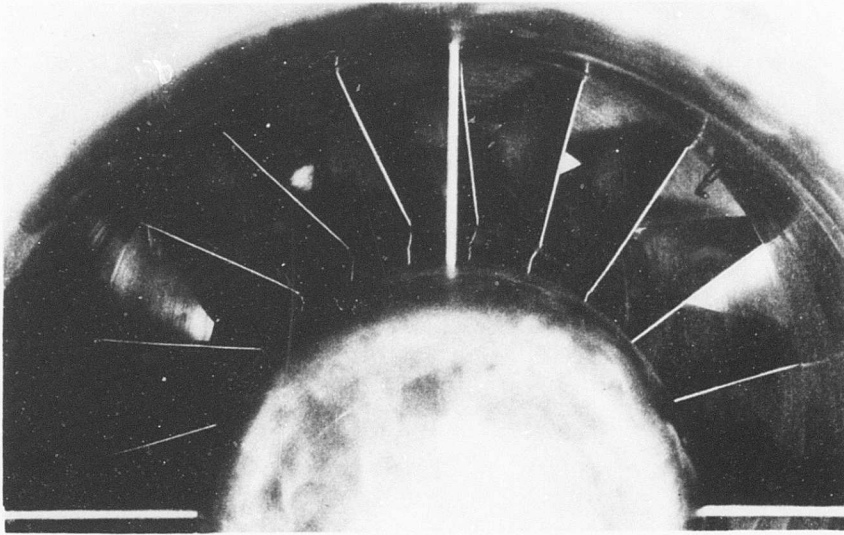
Figure 3. Semi-Reverse-Flow Separator Inlet.

Airflow
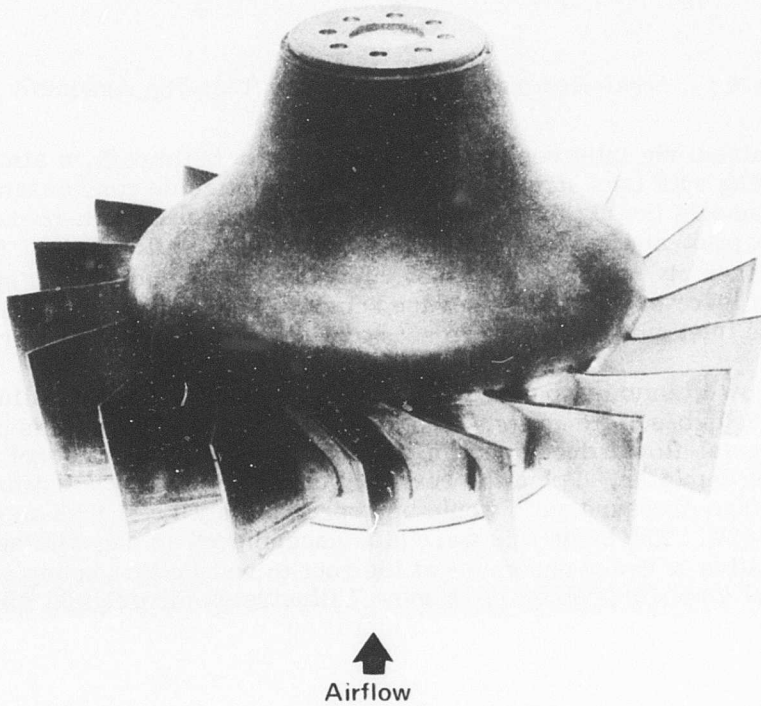
Figure 4. Semi-Reverse-Flow Separator Swirl-Vane Assembly.

Inlet Air

Scavenge
Discharge

Scavenge
Discharge

Clean Air
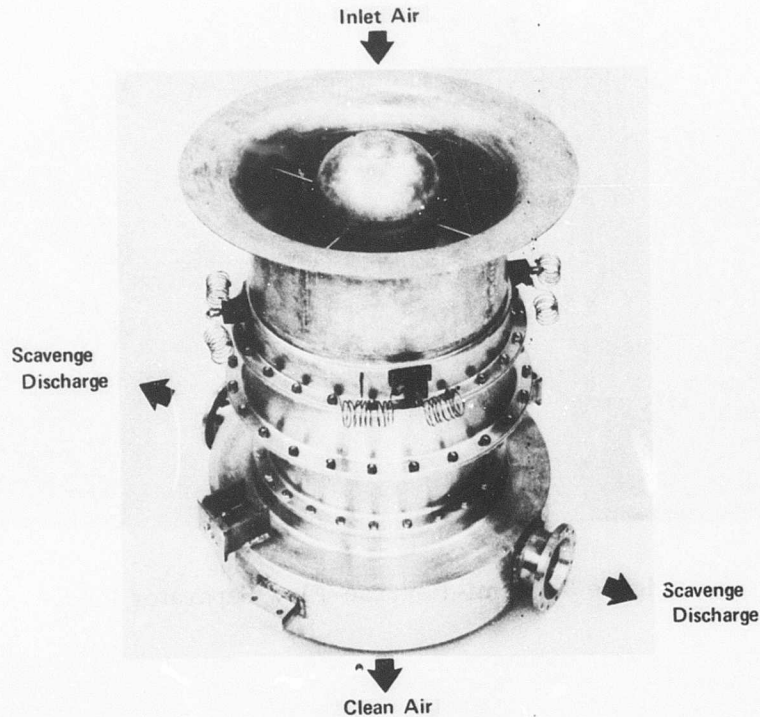
Figure 5. Semi-Reverse-Flow Separator Test-Rig Assembly.

The all-aluminum rig inlet section is comprised of a bellmouth, a simulated
bearing housing with four struts, and a variable inlet guide vane assembly. The
bellmouth connects the rig to the test facility dust-feeder screen-basket assembly.
A total of six pitot-static probes in the inlet provide inlet flow data. The inlet
guide vane assembly consists of 12 movable vanes connected with a "sync" ring
actuated by a lever arm outside the vane housing. Throughout the entire test
program, the inlet guide vanes were set at 20 deg nominal midspan prewhirl.

The mixed-flow titanium impeller was obtained by modifying an existing impeller
sized for an 8.0-lb/sec flow rate. The mixed-flow configuration was produced
by using the axial-flow inducer section and a portion of the centrifugal flow section
of the existing impeller. From the resulting cutoff point, it was estimated that
the overall stage pressure ratio would be approximately 1.7:1 with an estimated
efficiency of 82%. The blade tips were also uncambered 15 deg with approximately
a linear variation to 0-deg uncamber at the root to reduce tip loading and mini-
mize potential stability problems. Figure 7 illustrates the original full-size im-
peller and the resulting mixed-flow configuration.

6
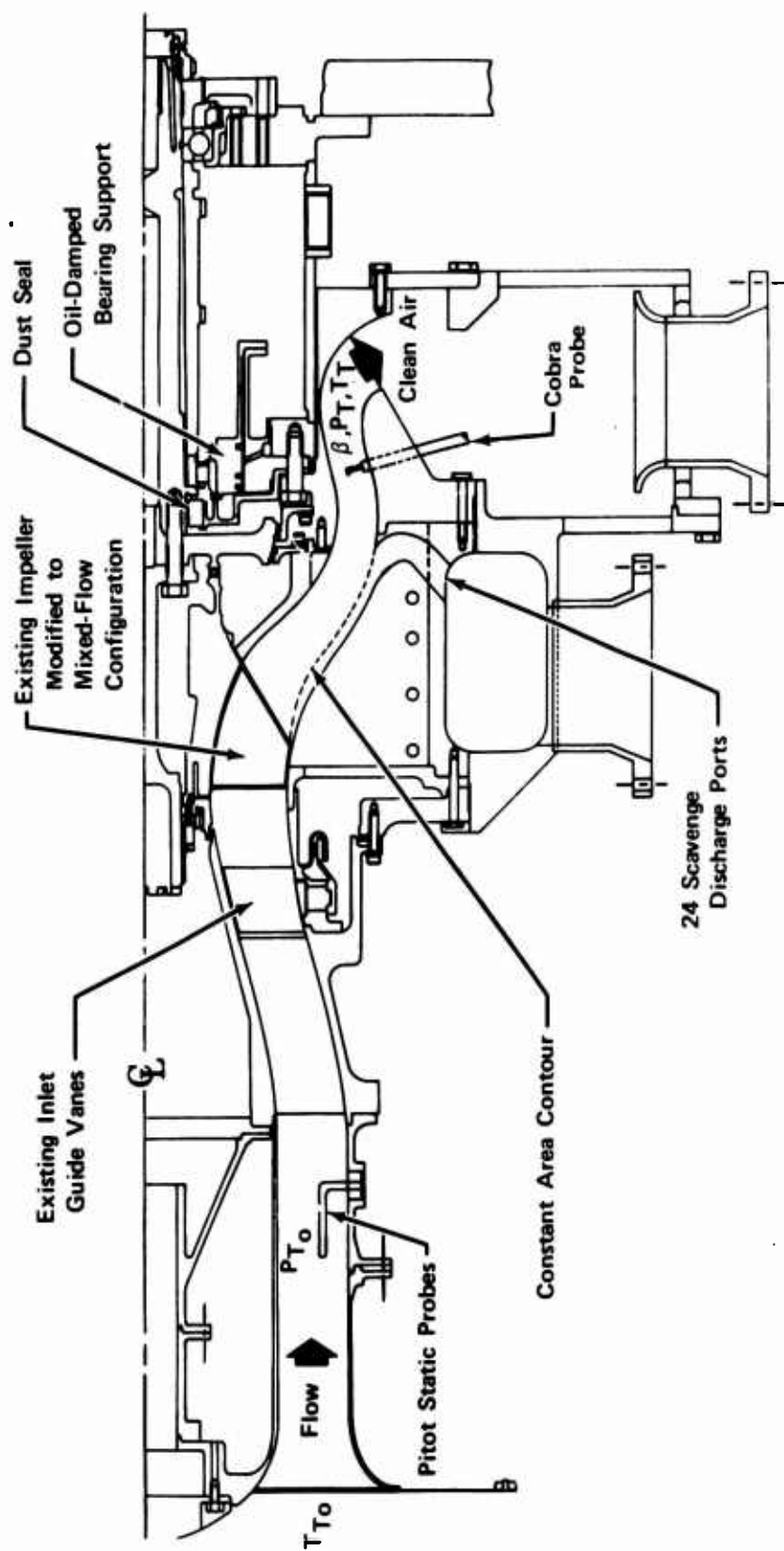
Figure 6. Powered Mixed-Flow Particle Separator Schematic.
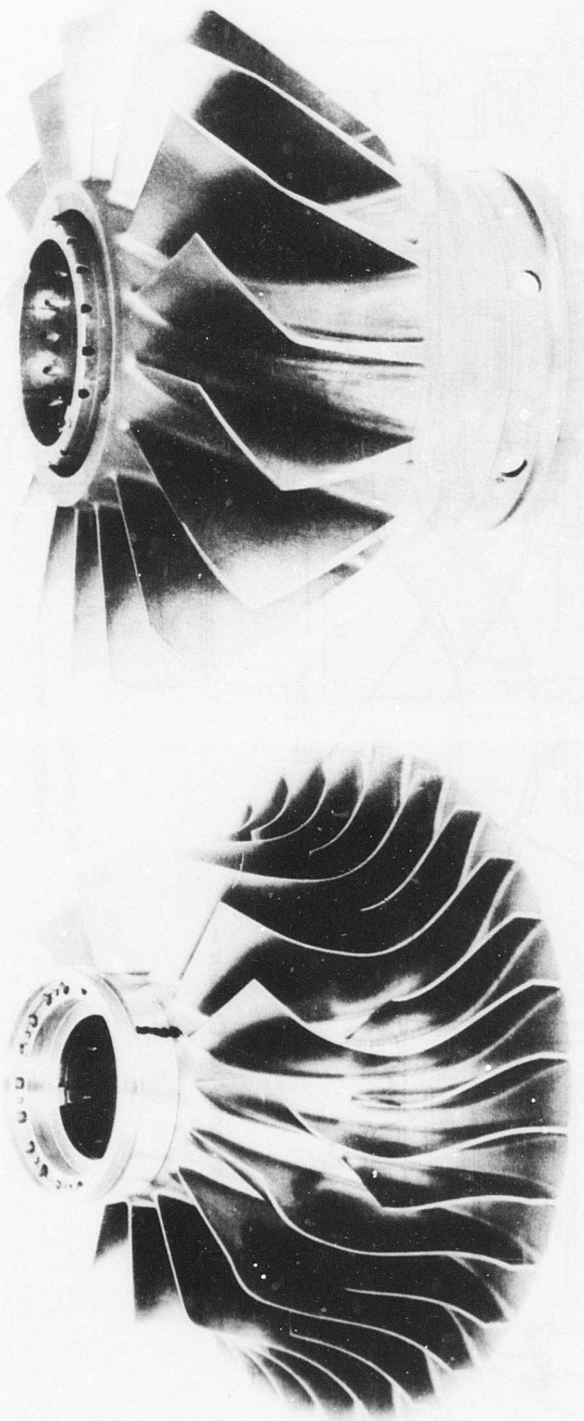
Before

After

Figure 7. Comparison of Original Full-Size Impeller and Mixed-Flow Configuration.

8

The aluminum shroud section was made as a split assembly so that it could be tested with a constant-area contour and then readily removed for final machining of the particle scavenge zone while the rig was on the test stand. To substantiate the particle trajectory computer program prediction of the scavenge zone location, the shroud contour was initially painted so that a brief test of dust ingestion would wear areas of concentrated particle impaction. The shroud was made with provisions for 24 scavenge discharge ports that would align with the final scavenge zone contour. Figure 8 shows the impeller and constant-area contour assembly with the split shroud in place. Figure 9 shows the same view after the final scavenge-zone contour had been machined. It can be seen that the 24 scavenge discharge ports were located so as to align with the swirling flow from the mixed-flow impeller.

The rig uses a special bearing system designed for high-speed compressor rig testing. It includes an oil-damped bearing support, which reduces bearing vibrational loads, and a carbon seal package designed to keep dust out of the bearing housing. Both the front and rear bearings were instrumented with thermocouples, and the bearing support was instrumented with accelerometers for monitoring bearing vibrational loads. Required axial thrust loads were maintained by pressurizing a thrust-balance piston within the bearing housing.

Impeller discharge flow conditions were monitored downstream of the scavenge zone splitter with a traversing cobra probe, which measures total pressure, total temperature, and swirl angle. The completed assembly of the powered mixed-flow separator test hardware is shown in Figure 10.

9

Airflow
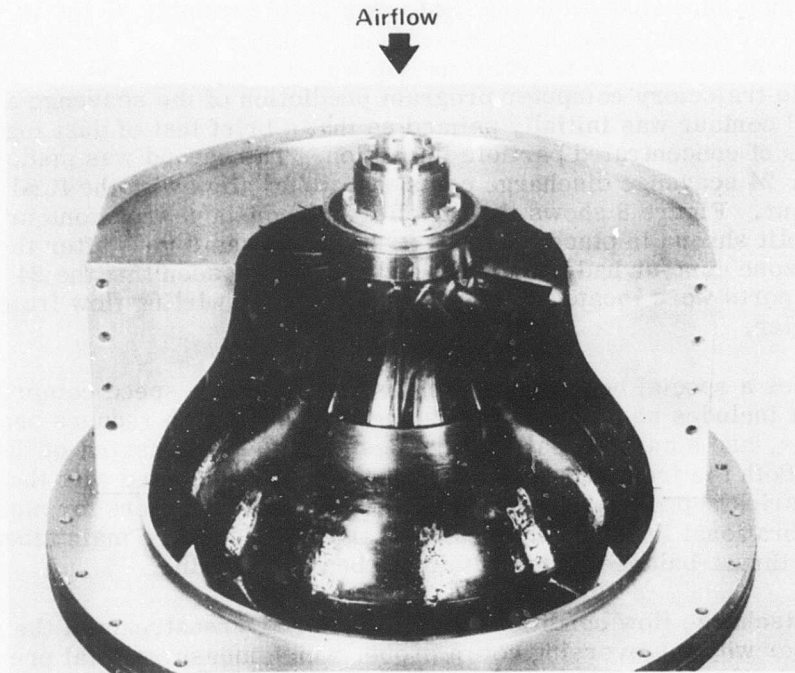
Figure 8. Assembly of Impeller and Constant-Area Contour
Split Shroud.

Airflow

Figure 9. Assembly of Impeller and Final Scavenge-Zone
Contour Split Shroud.

10

Inlet Air

Scavenge
Discharge

Clean Air

Clean Air
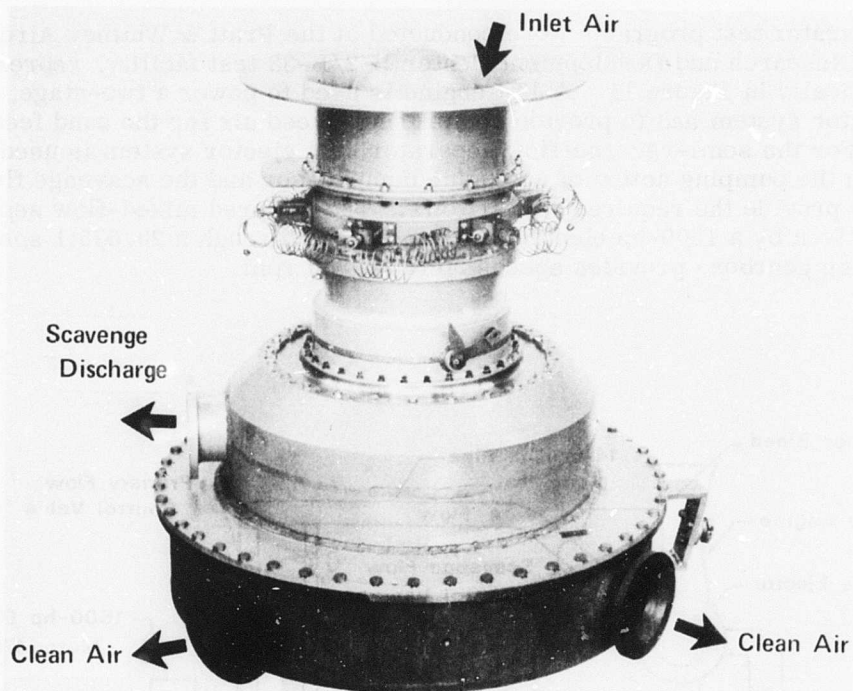
Figure 10. Powered Mixed-Flow Separator Test Rig Assembly.

Test Facility

The separator test programs were conducted at the Pratt & Whitney Aircraft Florida Research and Development Center B-2/B-33 test facility, represented schematically in Figure 11. A JT4 engine is used to power a two-stage, exhaust-gas ejector system and to provide compressor-bleed air for the sand feed equipment. For the semi-reverse-flow separator, the ejector system is used to simulate both the pumping action of an engine compressor and the scavenge flow potential and thus provide the required rig airflows. The powered mixed-flow separator rig is driven by a 1500-hp electric motor, which, through a 20.675:1 speed-increasing gearbox, provides speeds up to 36,500 rpm.
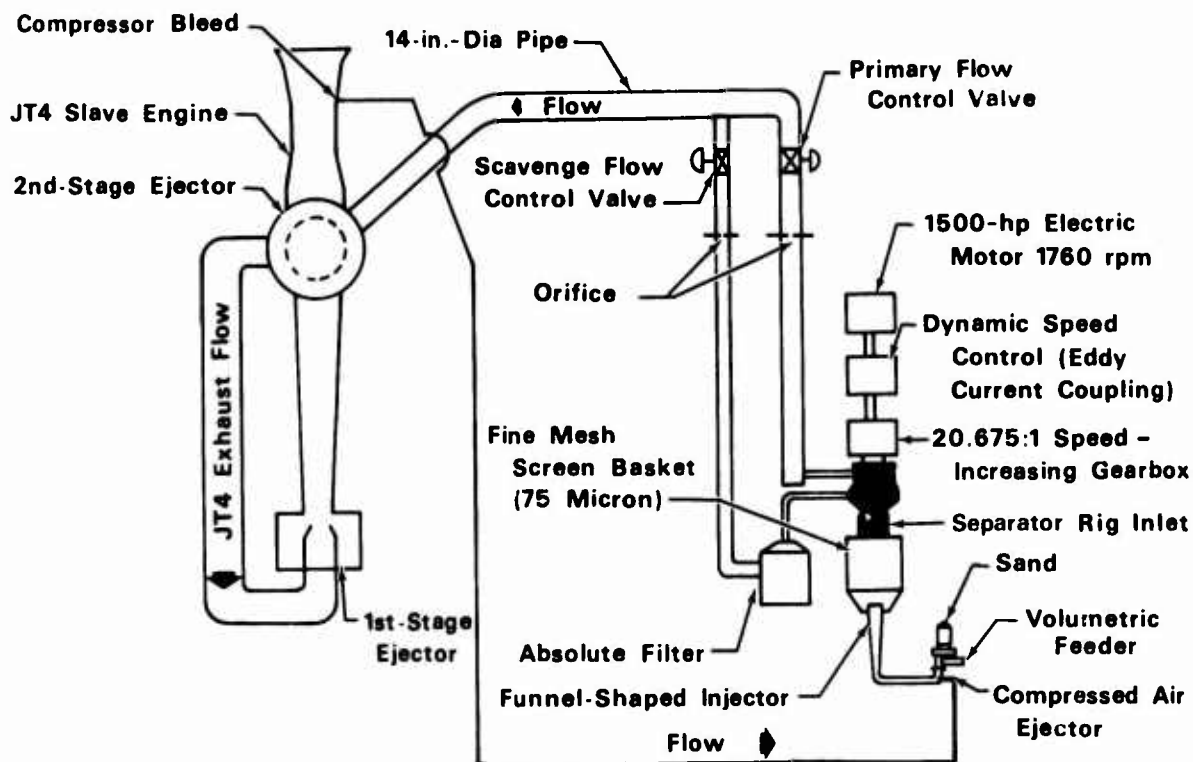
Figure 11. Facility Schematic for Separator Test Program.

The sand feed system is a copy of the system developed by the Aeronautical Engine Department at the Naval Air Propulsion Test Center. This system consists of a sand hopper and feeder, an ejector duct system, and a fine-mesh screen basket around the rig inlet. The feed system is shown in Figure 12. Storage and metering of the sand were accomplished with a BIF Industries Model 22-01 volumetric disc feeder, shown in Figure 13, mounted on the test stand near the rig. Prior to testing the semi-reverse-flow separator, the feeder was calibrated to determine its dust feed rate in lb/hr of AC coarse test dust as a function of transmission speed setting, and to check repeatability. A plot of these data, Figure 14, was used in conjunction with a curve of rig flow (lb/hr) vs dust flow (lb/hr) at a concentration of 0.015 gm/ft^3 to set the required dust flow rate at the various air flow rates. Prior to testing the powered mixed-flow separator, the feeder was check-calibrated and found to be within 1.0% of the initial calibration. These data are shown on Figure 14. To keep the test dust in the hopper from caking and forming lumps due to atmospheric moisture, a 150-w electric strip heater was mounted on the inside of the hopper curve.

The ejector duct system carries dust from the feeder to the screen basket. From the feeder the dust flows by gravity into the ejector bin, where JT4 compressor-bleed air is supplied. Air pressure and temperature at the ejector were 20 psia and approximately 150°F. Dust flows from the ejector bin through a 4-in.-diameter rubber hose to a funnel-shaped diffuser located at the screen basket.
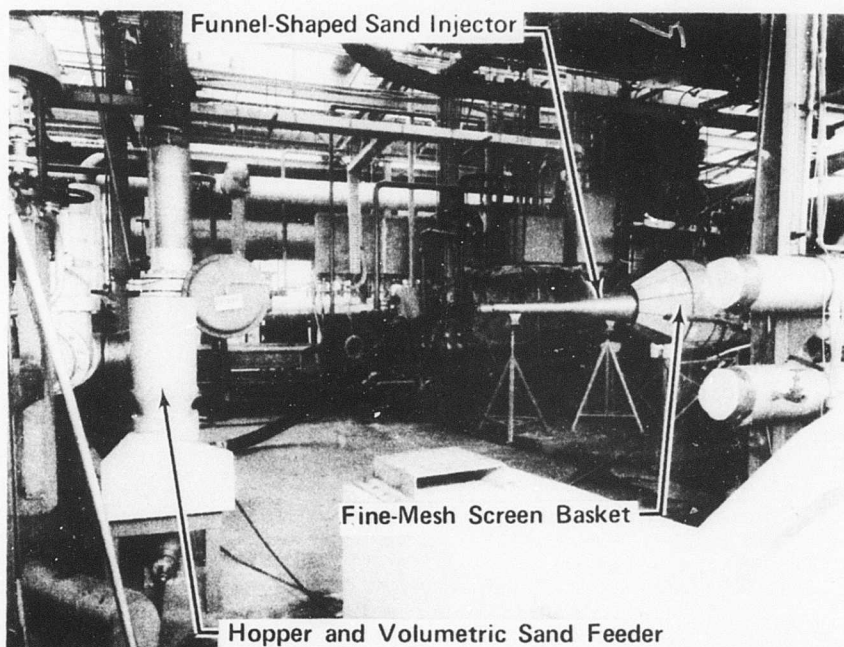
Figure 12. Sand Feed System for Separator Test Program.
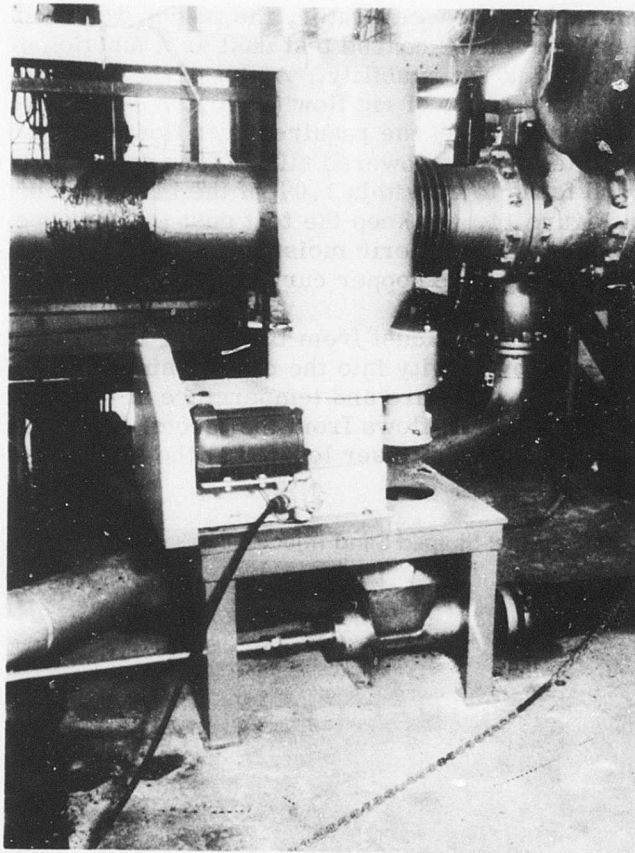
Figure 13. BIF Industries Volumetric Disc Feeder.

14
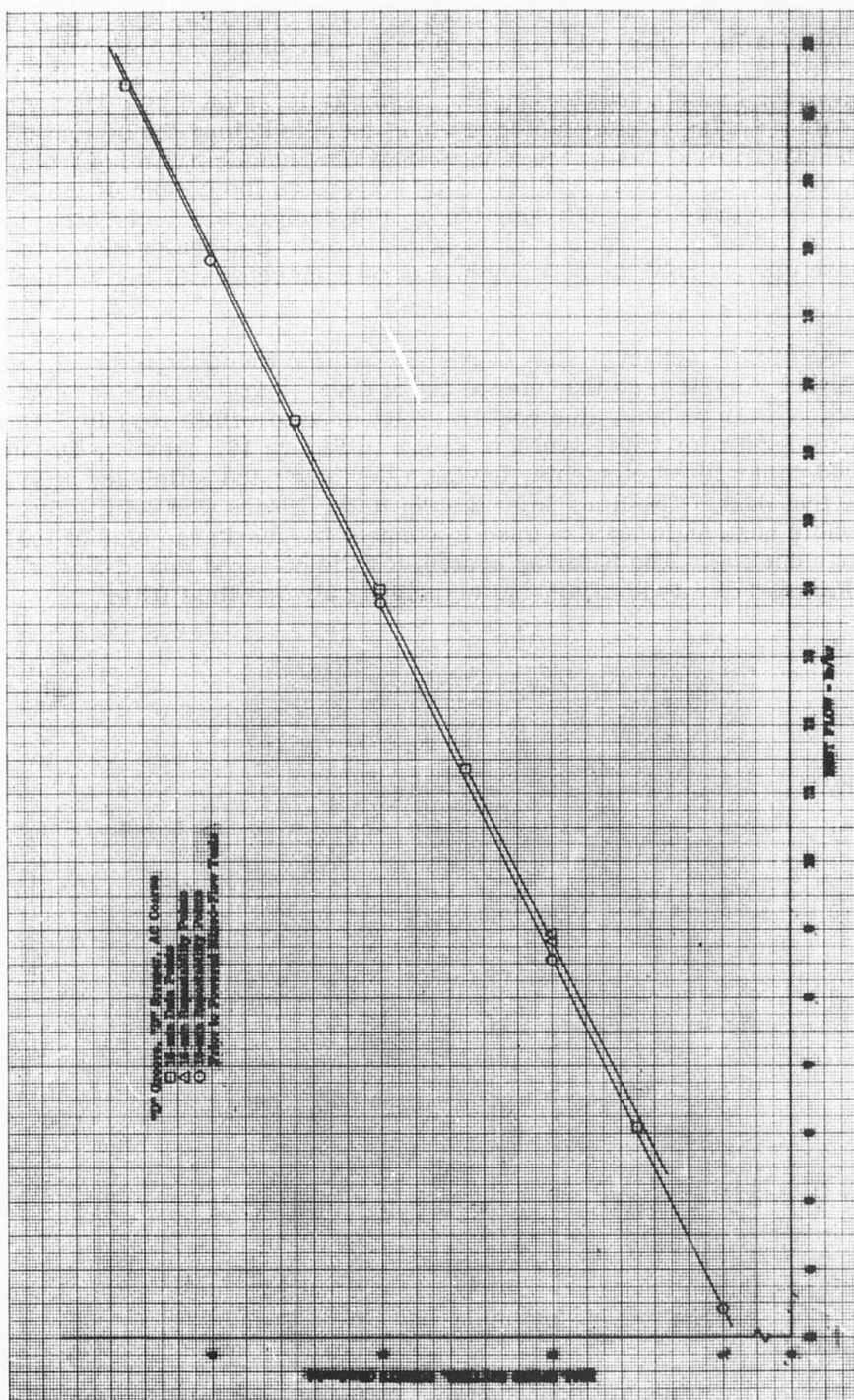
Figure 14. Volumetric Disc Feeder Calibration Curve.

The inlet screen basket, shown in Figure 15, was constructed from type 304 stainless steel, twilled dutch weave filter cloth with 75μ openings, and spot welded to the inside of a light-weave frame made of 3/8-in.-diameter solid rod. The dust cloud leaving the sand ejector system enters and is contained by the screen basket, ensuring that all dust leaving the feeder is ingested by the rig. An air manifold with a series of side-facing holes is installed along the bottom of the screen basket to provide an air curtain to keep the heavier particles from settling out of the air stream and becoming trapped on the bottom of the basket. Air for this air manifold is also supplied by JT4 compressor bleed air. The rear of the screen basket has a special plate with six over-the-center clamps welded to it. These clamps hold the bellmouth inlet of each separator rig to the screen basket.

Dust collected in the scavenge flow of each separator was ducted through an absolute filtering system so that the weight of dust separated per test could be determined. Filter weight gains could be measured to within ±0.1 lb. The semi-reverse-flow separator filter system, shown in Figure 16, uses two Donaldson EBA15-0003 paper filter elements, having a demonstrated efficiency of 99.953% on AC fine test dust. The lines from the rig to the filters was 4-in.-diameter reinforced flexible hose and was also used to connect the discharge side of the filters to the scavenge ducting. The filtering system for the powered mixed-flow separator, shown in Figure 17, was similar, but employed only one final filter.
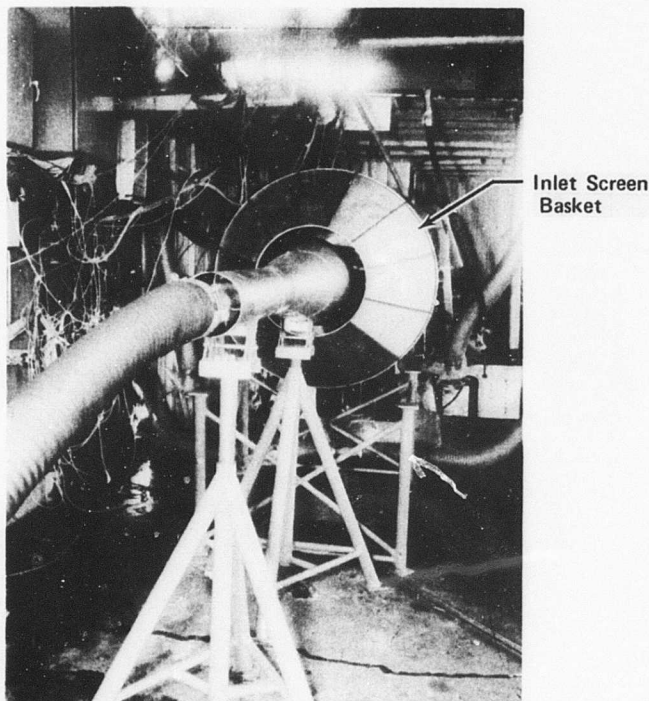
Figure 15. Ejector Duct System, Diffuser, and Inlet Screen Basket.

16

Semi-Reverse-Flow Separator ─

Absolute Filters ─
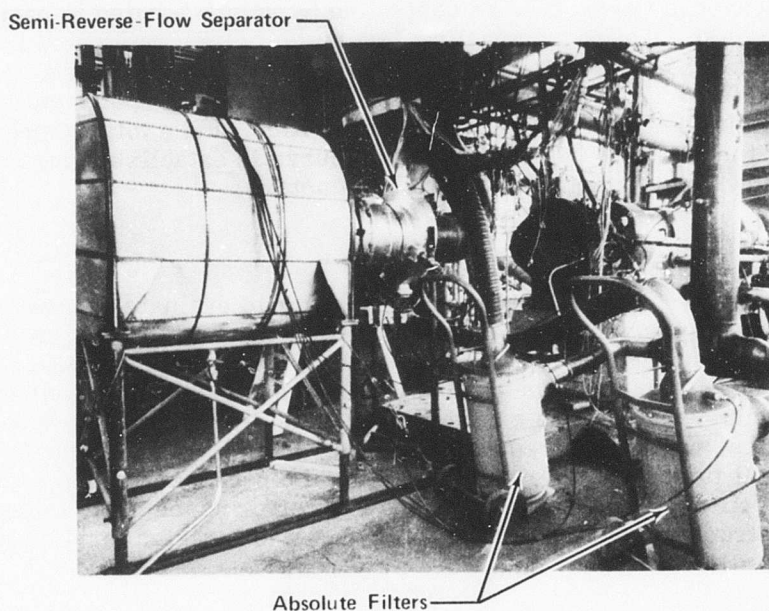
Figure 16. Semi-Reverse-Flow Separator Scavenge Filter System.

Powered Mixed-Flow Separator ─

Absolute Filter ─
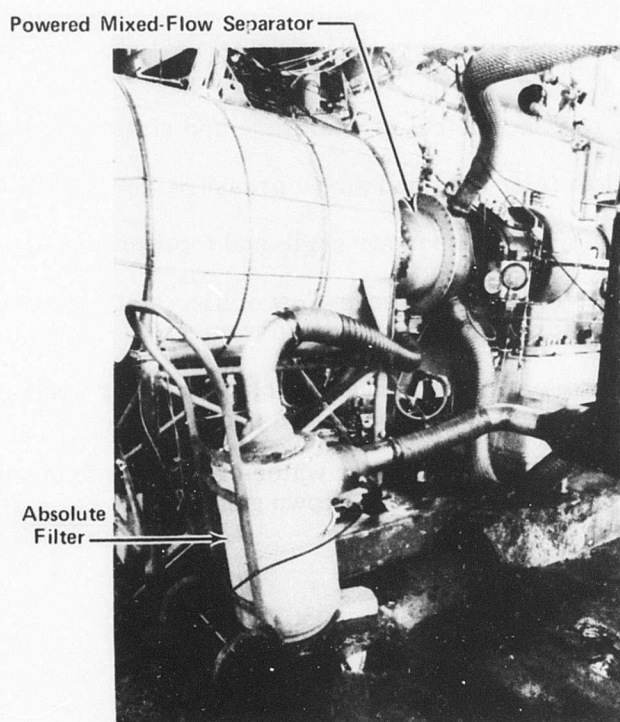
Figure 17. Powered Mixed-Flow Separator Scavenge Filter System.

17

Primary and scavenge flow rates are controlled by valves located in each flow pipe, as shown on the facility schematic, Figure 11. Orifices located in each line were made to ASME standards, and, although not test-calibrated, flows are accurate to within 2%. Each orifice is instrumented with an upstream static pressure, a differential static pressure across the orifice, and a total temperature downstream of the orifice. A theoretical flow curve is established for each orifice depending on flow pipe diameter and orifice diameter.

Test Procedure

The primary objectives of the testing program were to evaluate separation efficiency, aerodynamic performance characteristics, and operation in rain and foliage-ingestion conditions for both particle separators. The nominal test conditions are listed in Table I. The testing procedure basically involved setting the correct primary and scavenge air flow rates and then recording aerodynamic performance data, which required about 15 min. This involved manually reading and recording all flow parameters and obtaining the necessary cobra probe traverse data. After obtaining the aerodynamic performance data, the cobra probes were retracted from the airflow, and dust was ingested for 45 min during which the separation efficiency data were acquired.

The first series of tests with the semi-reverse-flow separator was conducted with the 30-deg nominal swirl vanes installed. After starting the JT4 slave engine, flow rates were set by adjusting the primary-flow and scavenge-flow control valves to obtain the desired flow rates through the rig. The flow rates set were corrected to sea level standard conditions. Once the flow rates were established, the recording of the steady-state aerodynamic performance data was initiated. The parameters measured were:

1. Screen basket ambient temperature and static pressure

2. Bellmouth inlet total and static pressure (four each)

3. Scavenge duct midspan air angle and total pressure (cobra probe)

4. Primary-flow and scavenge-flow orifice static pressure, differential pressures, and temperatures

5. Equivalent-engine compressor-inlet-plane air angle and total pressure at five positions (cobra probe).

All pressures were monitored on either water or mercury manometers, and temperatures were read out on a vertical Brown gage.

18

TABLE I. NOMINAL TEST CONDITIONS

Semi-Reverse-Flow Separator

Test Time (hr)	Nominal Primary/Scavenge (% Flow)	Primary Flow (lb/sec)	Scavenge Flow (lb/sec)	Nominal Swirl (deg)	Test Objective
0.25	100%/40%	8.00	3.20	30	Aerodynamic performance
0.75	100%/40%	8.00	3.20	30	Separator efficiency
0.25	80%/40%	6.40	2.56	30	Aerodynamic performance
0.75	80%/40%	6.40	2.56	30	Separator efficiency
0.25	60%/40%	4.80	1.92	30	Aerodynamic performance
0.75	60%/40%	4.80	1.92	30	Separator efficiency
0.25	100%/20%	8.00	1.60	30	Aerodynamic performance
0.75	100%/20%	8.00	1.60	30	Separator efficiency
0.33	100%/40%	8.00	3.20	30	Rain ingestion
0.33	100%/40%	8.00	3.20	30	Foliage ingestion
0.33	100%/40%	8.00	3.20	30	Aerodynamic performance
0.25	100%/40%	8.00	3.20	0	Aerodynamic performance
0.75	100%/40%	8.00	3.20	0	Separator efficiency
0.25	60%/40%	4.80	1.92	0	Aerodynamic performance
0.75	60%/40%	4.80	1.92	0	Separator efficiency

Powered Mixed-Flow Separator

Test Time (hr)	Nominal Primary/Scavenge (% Flow)	Primary Flow (lb/sec)	Scavenge Flow (lb/sec)	Scavenge Capability	Test Objective
0.10	100%/0%	8.00	0.00	No	Scavenge zone verification
0.90	100%/0%	8.00	0.00	No	Aerodynamic performance
0.25	100%/5.0%	8.00	0.40	Yes	Aerodynamic performance
0.75	100%/5.0%	8.00	0.40	Yes	Separator efficiency
0.25	80%/5.0%	6.40	0.32	Yes	Aerodynamic performance
0.75	80%/5.0%	6.40	0.32	Yes	Separator efficiency
0.25	60%/5.0%	4.80	0.24	Yes	Aerodynamic performance
0.75	60%/5.0%	4.80	0.24	Yes	Separator efficiency
0.25	100%/2.5%	8.00	0.20	Yes	Aerodynamic performance
0.75	100%/2.5%	8.00	0.20	Yes	Separator efficiency
0.25	100%/7.5%	8.00	0.60	Yes	Aerodynamic performance
0.75	100%/7.5%	8.00	0.60	Yes	Separator efficiency
0.33	100%/5.0%	8.00	0.40	Yes	Rain ingestion
0.33	100%/5.0%	8.00	0.40	Yes	Foliage ingestion
0.33	100%/5.0%	8.00	0.40	Yes	Aerodynamic performance

After the performance data had been obtained, the cobra probes were retracted
from the airflow and the flow control valves were closed so that the absolute filters
could be removed from the scavenge lines for weighing to obtain a clean tare
weight. After reinstalling the filters and setting the volumetric disc feeder to pro-
vide the correct concentration of AC coarse test dust, the flows were again set to
the desired corrected rates. A carefully timed test of 45 min was then made,
during which dust flow and both primary and scavenge flow rates were monitored.
After this timed period, the filters were reweighed and the weight of separated
dust had thus been determined. The filter elements were then cleaned and rein-
stalled, and the test procedure was repeated for the next test condition.

After completing the separation efficiency tests with the 30-deg nominal swirl
vanes, the test stand was prepared for the rain- and foliage-ingestion tests by
removing the dust feed diffuser from the screen basket. For the rain-ingestion tests,
a water hose and spray nozzle were set up in front of the screen basket. (See
Figure 18.) This arrangement provided a very uniform spray and was determined
to have a flow rate of 1.5 lb/sec. After establishing the 100%/40% test conditions,
a set of performance data was obtained. The simulated rain-ingestion test was
then conducted for 20 min, after which another set of performance data was ob-
tained.
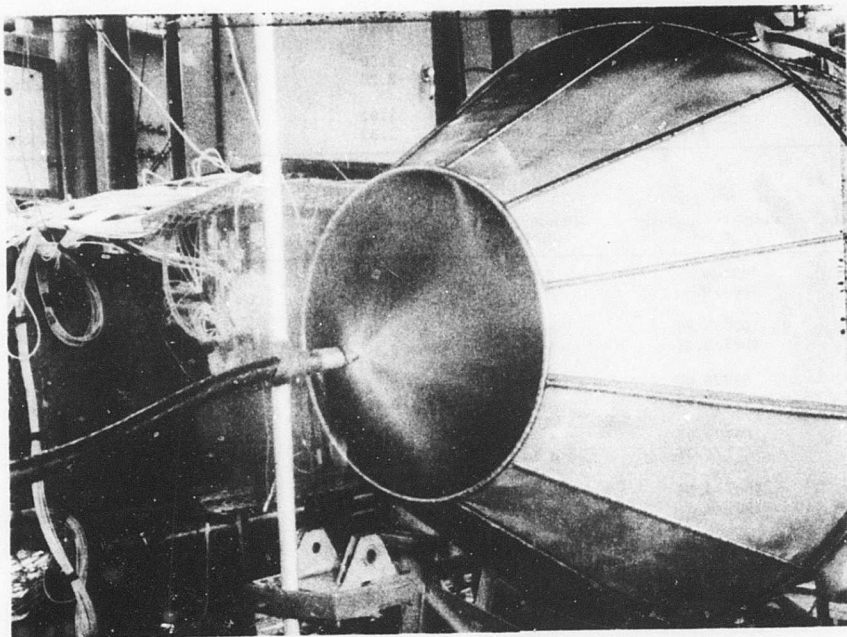
Figure 18. Water Spray Nozzle Setup for Simulated Rain-
Ingestion Test.

For the foliage-ingestion test, approximately 1.1 lb of dry straw was fed into the separator. A sample of this foliage is shown in Figure 19. The straw was first spread out in the bottom of the screen basket, and then the 100%/40% test condition was established. By slowly increasing the air pressure in the manifold in the bottom of the screen basket, the straw was slowly fluffed up and ingested by the separator. Another set of performance data was obtained upon completion of the foliage-ingestion test.

The remaining tests to be performed required replacing the swirl vanes with the no-swirl hub. The separator was then tested at two test conditions, 100%/40% and 60%/40%, at which both aerodynamic performance data and separator efficiency were determined. A foliage-ingestion test was then made, again using approximately 1.1 lb of dry straw.

No rig problems were encountered in the testing of the semi-reverse-flow separator; however, one error was found in the sand feed ejector system. After conducting the dust flow test at the 80%/40% test condition, an inspection of the test stand revealed a significant amount of dust had collected on top of the rig, behind the screen basket. This was apparently caused by too high a sand feeder ejector pressure, which was set at 40 psia for the first three tests. The high pressure was causing sand to be blown through the screen basket, thus causing an error in the determination of the separator efficiency. After experimentation, it was determined that a sand feeder ejector pressure of 20 psia would prevent sand from blowing through the screen basket. The 100%/40% and 80%/40% tests were then repeated, and all further tests were conducted at this lower ejector pressure.

NOT REPRODUCIBLE

Figure 19. Foliage Sample for Simulated Foliage-Ingestion Test.

Testing with the powered mixed-flow separator was somewhat more complex, since the high rotational speeds involved required close monitoring of bearing temperatures and vibration levels. Prior to beginning impeller rotation, it was necessary to set the thrust piston GN_2 pressure, which applies an axial thrust load to the impeller, the front- and rear-bearing oil jet pressures, and the bearing oil damper pressu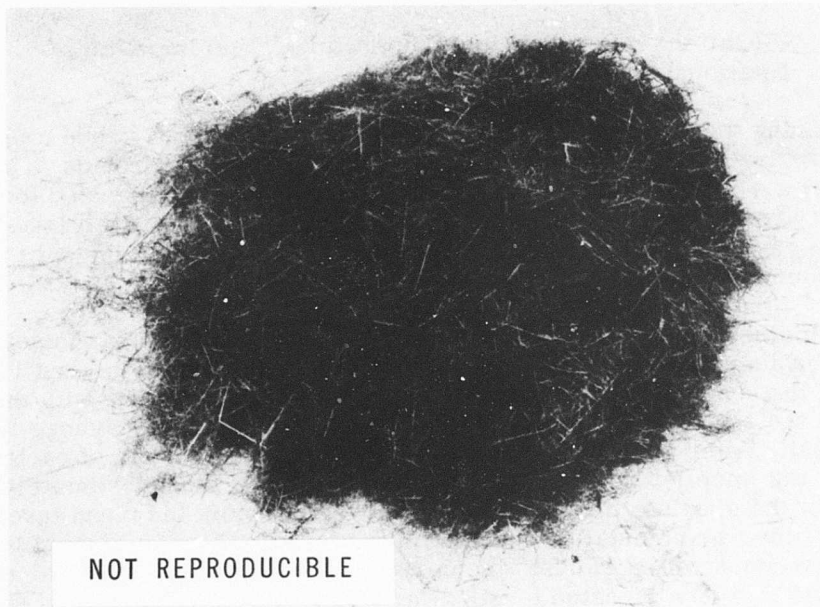re. Impeller rotation was then begun and rpm increased in increments of 5000/min. During this period, vibration levels were continuously monitored on G-meters and recorded on FM magnetic tape. A pause at each 5000-rpm increment also allowed bearing temperatures to stabilize.

Once the desired rotational speed had been reached, the JT4 slave engine was started, and the flow control valves were set to obtain the desired primary flow and scavenge flow. For the first test condition, there was no provision in the shroud for scavenge flow, so only the primary flow was set. The recording of the steady-state aerodynamic performance data was then initiated with the parameters measured being:

1. Screen basket ambient temperature and pressure

2. Bellmouth total and static pressures (six each)

3. Impeller discharge flow path air angle, total temperature, and total pressure at five positions (cobra probe)

4. Primary-flow orifice static pressure, differential pressure, and temperature

5. Vibration levels, bearing temperatures, and impeller rotational speed.

After obtaining the aerodynamic performance data, the cobra probe was retracted from the airflow, and the volumetric dust feeder was set to provide AC coarse test dust at a concentration of 0.015 gm/ft^3. Dust was then ingested for 0.1 hr for the purpose of locating the area of highest dust concentration on the shroud OD. The rig was then partially disassembled on the test stand, and the split shroud was removed for machining of the particle scavenge annulus.

After machining, the split shroud was reinstalled in the rig, and the scavenge line and absolute filter were connected to the rig scavenge port. (See Figure 17.) Testing of the separation efficiency of the rig was then initiated, with the run procedure the same as previously described, except that the scavenge flow rate was also set. After obtaining the aerodynamic peformance data at each airflow condition, the impeller rotational speed was decreased to approximately 15,000 rpm so that the absolute filter could be removed to obtain the clean tare weight. After the filter was reinstalled and the volumetric dust feeder was set to provide the proper concentration of dust, the correct flow rates and rotational speed were reset. Dust was then ingested for 45 min, while dust flow, rotational speed, and flow rates were monitored. After the timed period, the filter was reweighed to determine the weight of dust separated. After the filter element was cleaned, the above procedure was again followed until all of the separator efficiency tests were conducted.

22

During the first test at the 100%/5% flow condition, the run was aborted due to low thrust-piston pressure. Inspection of the rig revealed dust on the rig casing forward of the scavenge manifold, obviously leaking past the snap fit on the manifold. The manifold was removed and all joints were sealed with RTV, providing a good scavenge-flow manifold seal. It was also believed that a leak had developed in the primary airflow discharge duct, so it was decided to set rig flow by determining the airflow from the bellmouth inlet pitot-static probes. The inlet had been calibrated during the previous sand ingestion tests, so the curve from these data was used to determine the rig total airflow. Since a good seal was obtained in the scavenge flow, the scavenge flow orifice was used to set the required scavenge flow once the desired total inlet flow had been set. This technique was used for the remainder of the tests.

The simulated rain-ingestion test was conducted as previously described for the semi-reverse-flow separator. A water flow rate of 1.5 lb/sec was again used, and the spray nozzle setup was as shown in Figure 18. The 100%/5% test condition was set, and aerodynamic performance data were recorded. The simulated rain-ingestion test was then conducted for 20 min, after which another set of aerodynamic performance data was recorded. The foliage-ingestion test was then conducted using the identical procedure for the semi-reverse-flow separator. Approximately 0.8 lb of straw was ingested, after which another set of aerodynamic performance data was recorded.

Test Results

Both separators were tested with AC coarse test dust to determine separation efficiency and with water spray and foliage ingestion to evaluate operation in an adverse environment. Test results for both the semi-reverse-flow separator and the powered mixed-flow separator are plotted in Figure 20. Separation efficiency and pressure drop or rise are shown as a function of percentage of design airflow. At the design airflow condition of 8.0 lb/sec and 40% scavenge flow, the semi-reverse-flow separator demonstrated 88.5% separation efficiency with an average pressure drop of 2.8 in. H_2O. At the design airflow, the powered mixed-flow separator demonstrated a maximum separation efficiency of 58.7%, with 8.4% scavenge flow and an average pressure rise of 6.8 psi (at the test condition achieved, i.e., 94% of design flow).

A chronological summary of the semi-reverse-flow separator test data is given in Table II. The primary and scavenge airflow rates have been corrected to sea level standard conditions. The separator average pressure drop was determined by area-averaging the five cobra-probe total pressures obtained during each condition and subtracting the bellmouth inlet total pressure from them; the profiles are presented in Figure 21. The average swirl angle at each test condition was also determined by the area-averaging method, with Figure 22 showing the swirl profiles obtained at each test condition. The dust separation efficiency, as a percentage of dust, by weight, separated from the total separator flow, was obtained by weighing the absolute filters before and after each dust flow test and by comparing the weight gain to the total weight of dust fed into the separator. The actual dust concentration was derived by dividing the total separator dust flow per unit time by the actual volume of total separator airflow per unit time.
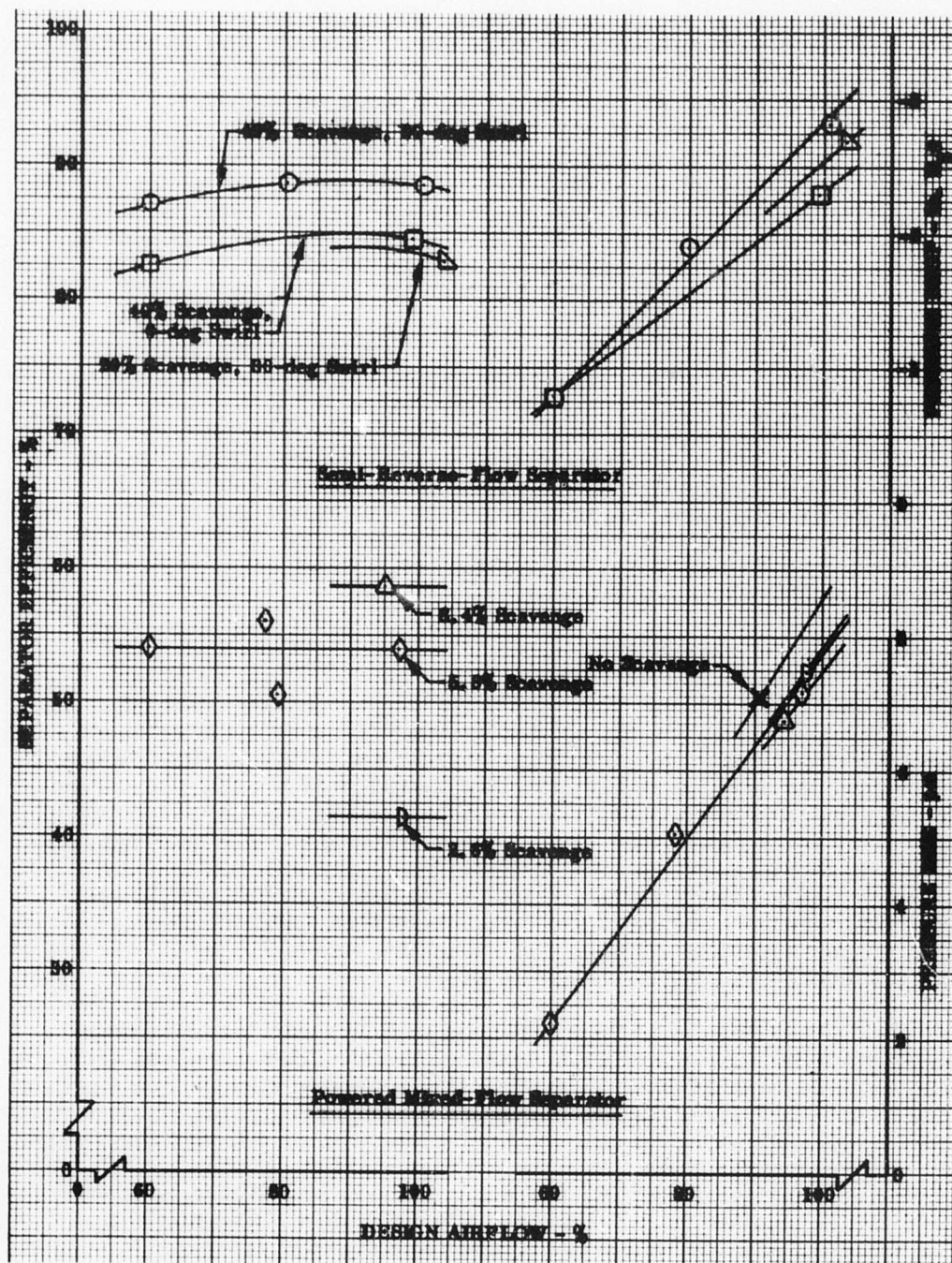
Figure 20. Summary of Test Results From Separator Test
Program.

TABLE II. SEMI-REVERSE-FLOW SEPARATOR TEST RESULT SUMMARY

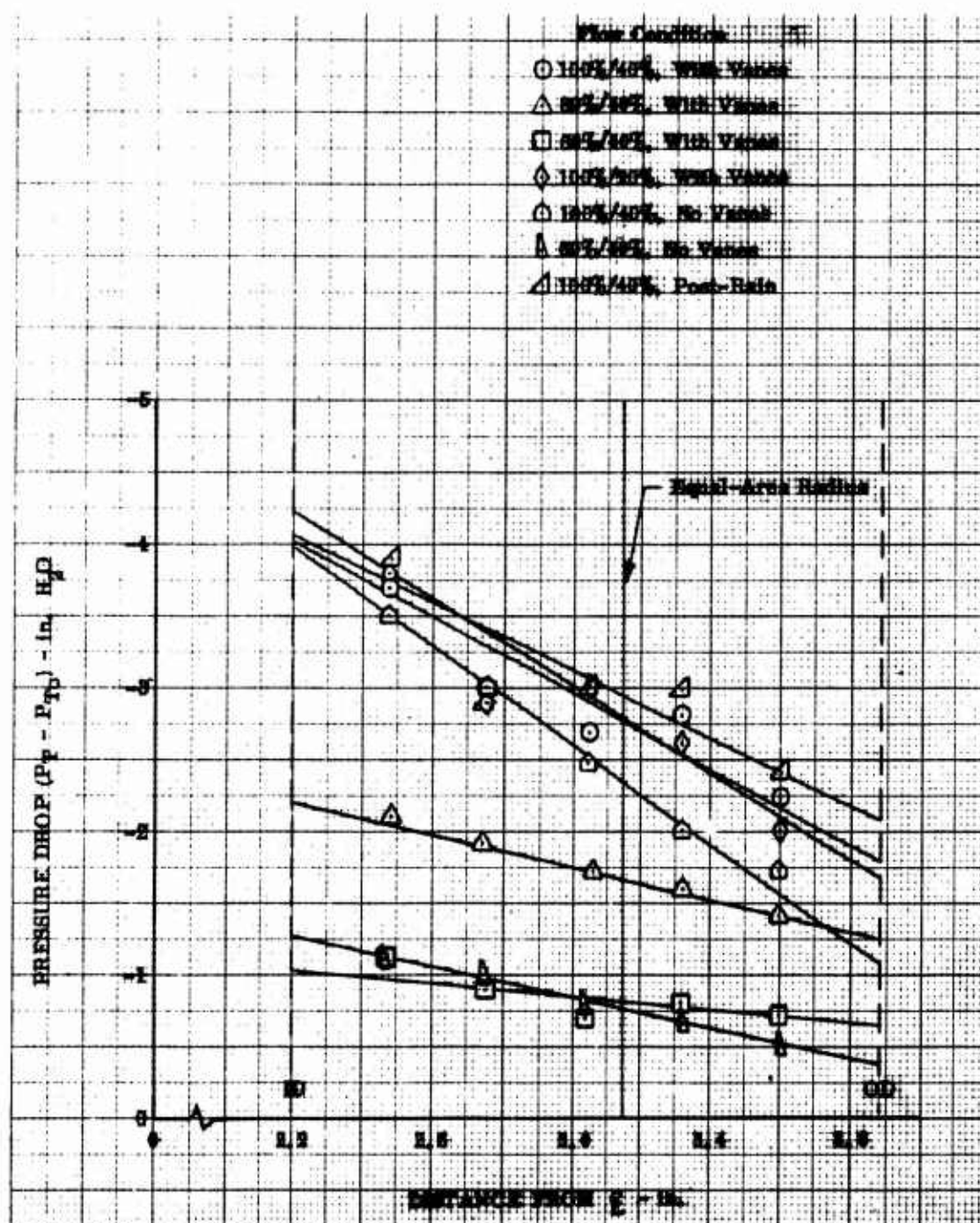| Nominal Primary/Scavenge (% Flow)	Type of Test	Test Time (min)	Primary Airflow (lb/sec)	Scavenge Airflow (lb/sec)	Primary Airflow (% Design)	Scavenge Airflow (% Primary)	Average ΔP Pressure Drop (in. H_2O)	Average Swirl Angle, 90-deg = Axial	Dust Separation Efficiency (%)	Actual Dust Concentration (%) (gm/ft³)	Remarks
100%/40%	Performance	15	8.03	3.18	100.4	39.6	2.8	65	-	-	Test terminated prematurely due to unscheduled JT4 shutdown.
100%/40%	Sand Ingestion	38	7.98	3.18	99.8	39.8	-	-	87.9	0.0143	
100%/40%	Sand Ingestion	45	8.06	3.19	100.8	39.6	-	-	88.1	0.0142	Repeat of above 100% 40% test.
90%/40%	Performance	15	6.38	2.62	79.8	41.1	1.9	64	-	-	
80%/40%	Sand Ingestion	45	6.43	2.61	80.4	40.6	-	-	70.3	0.0144	Sand feed ejector pressure too high.
80%/40%	Sand Ingestion	45	6.46	2.63	80.3	40.7	-	-	88.6	0.0146	Repeat of 80% 40% test with reduced sand feed ejector pressure.
60%/40%	Performance	15	4.61	1.97	60.1	41.0	0.8	63	-	-	
60%/40%	Sand Ingestion	45	4.80	1.96	60.0	40.8	-	-	86.9	0.0142	Valid test.
100%/40%	Sand Ingestion	45	8.03	3.17	100.4	39.5	-	-	88.5	0.0145	Repeat of 100% 40% test with reduced sand feed ejector pressure.
100%/20%	Performance	15	8.24	1.68	103.0	20.4	2.7	70	-	-	
100%/20%	Sand Ingestion	45	8.30	1.67	103.8	20.1	-	-	83.0	0.0141	Valid Test.
100%/40%	Performance	20	8.25	2.85	103.1	34.5	2.8	65	-	-	Ingestion base performance test.
100%/40%	Post-Rain Performance	20	8.11	3.19	101.4	39.3	2.9	65	-	-	Post-rain ingestion performance test.
100%/40%	Post-Foliage	20	6.13	2.46	76.6	40.1	-	-	-	-	Post-foliage ingestion performance test over-ranged manometers.
					Swirl Vanes Removed						
100%/40%	Performance	15	7.93	3.15	99.1	39.7	2.3	94	-	-	
100%/40%	Sand Ingestion	45	7.94	3.13	99.3	39.4	-	-	84.4	0.0145	Valid Test.
60%/40%	Performance	15	4.81	1.95	60.1	40.5	0.8	94	-	-	
60%/40%	Sand Ingestion	45	4.77	1.89	59.6	39.6	-	-	82.4	0.0144	Valid Test.

Figure 21. Semi-Reverse-Flow Separator Total Pressure Drop
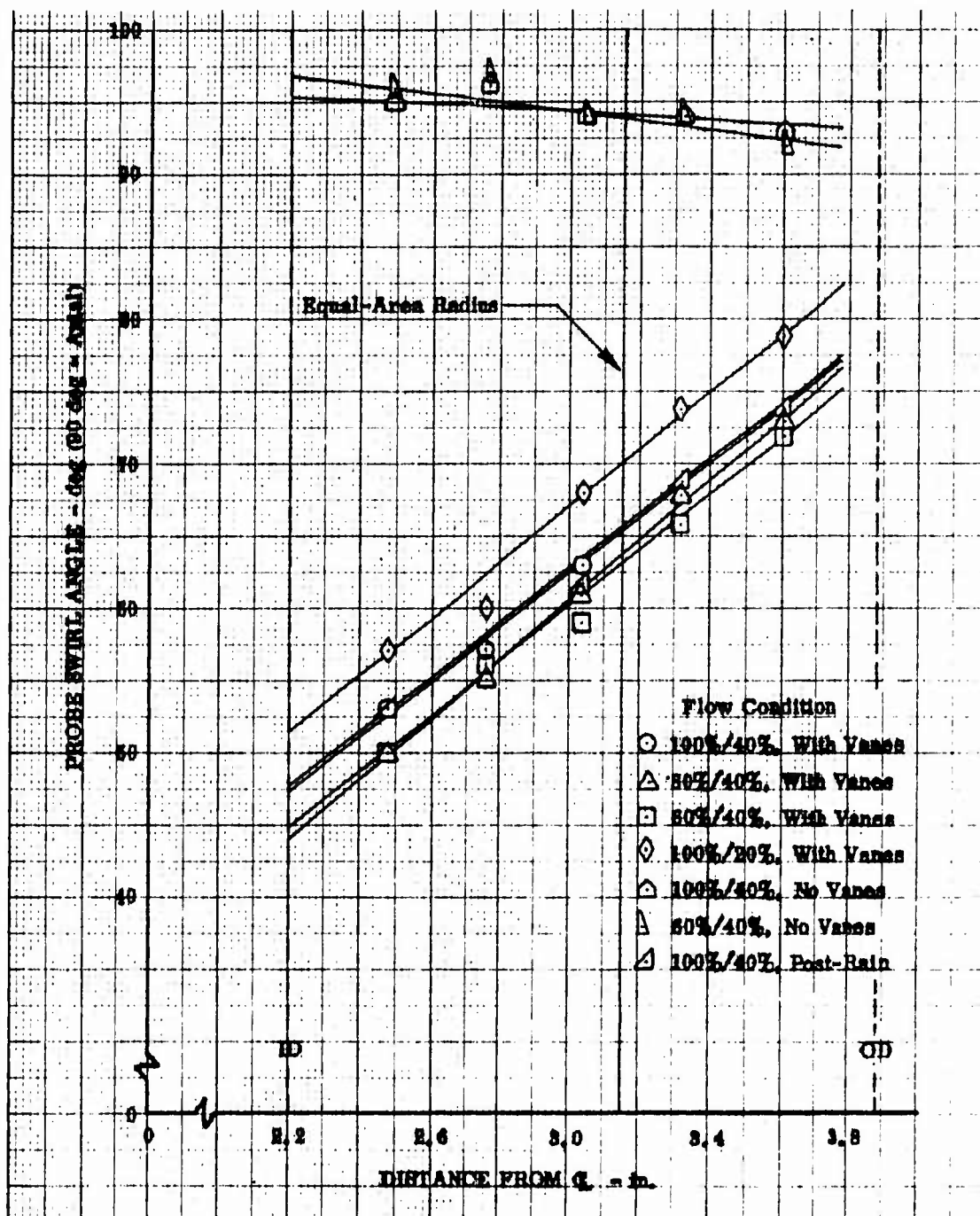Profiles at Various Test Conditions.

26

Figure 22. Semi-Reverse-Flow Separator Swirl Profiles at
Various Test Conditions.

At the design primary airflow test condition of 8.0 lb/sec and 40% scavenge flow, the semi-reverse-flow separator had an average pressure drop of 2.8 in. H_2O. This pressure loss was considerably less than the estimated loss of 6 in. H_2O derived in Phase I of this program. An investigation was made into the method of estimating the semi-reverse-flow separator pressure losses. The largest source of error was found to be in estimating the loss coefficient for the flow region from the Coanda ramp to the flow splitter. Since this particular flow situation was unfamiliar, a highly conservative loss coefficient was assumed, which, when coupled with the large flow area in this region, accounted for an excessive estimated total pressure loss.

After completing the aerodynamic-performance and separation-efficiency tests with the nominal 30-deg swirl vanes, the simulated rain-ingestion test was conducted at the 100%/40% test condition. The spray nozzle setup was as shown in Figure 18, with a spray rate of 1.5 lb/sec. There was no resultant effect on the separator due to water ingestion, as both pressure drop and swirl angle remained virtually unchanged from the base performance test. The foliage-ingestion test was then simulated, as previously explained in the Test Procedure section. Approximately 1.1 lb of straw was ingested by the separator, most of which collected on the 18 swirl vanes, as shown in Figure 23. The straw collection greatly increased the pressure drop in the separator--in excess of 40 in. H_2O.

The swirl vanes were then removed, and aerodynamic performance and separation efficiency tests were conducted at two airflow conditions for the no-swirl configuration. At the 100%/40% airflow condition, the no-swirl semi-reverse-flow separator configuration demonstrated a separation efficiency of 84.4% at a pressure drop of 2.3 in. H_2O. This is a 4.1 percent loss in separation efficiency over the 30-deg nominal swirl configuration, with a 0.5-in. H_2O reduction in pressure drop. Another foliage ingestion test was then conducted, also at the 100%/40% flow condition. Approximately 1.1 lb of dry straw was again used, but this time most of the straw passed through the separator, with a small amount collecting on the inlet struts as shown in Figure 24. A post-test visual inspection was made of the semi-reverse-flow separator hardware, revealing no apparent wear of the swirl vanes or separator flow passages.

A chronological summary of the powered mixed-flow separator test data is presented in Table III. The primary and scavenge air flow rates were again corrected to sea level standard conditions. The average pressure rise at each test condition is obtained by area-averaging the five total pressure measurements, taken across the primary flowpath downstream of the scavenge zone, to obtain an absolute total pressure, from which the average bellmouth inlet absolute total pressure was subtracted. The cobra probe total pressure profiles are shown in Figure 25. The average swirl angle at each test condition was obtained by area-averaging the five swirl angles measured across the flow passage. Figure 26 shows the swirl profiles obtained. The average total temperature is a numerical average of the five total temperatures obtained at the corresponding total pressure swirl-angle positions. Separation efficiency and the actual dust concentration at each test condition were determined as before with the semi-reverse-flow separator. Compressor aerodynamic efficiency was determined from the standard pressure-temperature relationship:

$$\eta = \frac{\left(\dfrac{P_T}{P_{To}}\right)^{\frac{\gamma-1}{\gamma}} - 1}{\left(\dfrac{T_T}{T_{To}}\right) - 1}$$

where

P_T = cobra probe total pressure (psia)

P_{To} bellmouth inlet total pressure (psia)

T_T cobra probe total temperature (°R)

T_{To} = bellmouth inlet total temperature (°R)

The test data were further analyzed to determine the characteristics of the mixed-flow impeller. A map of impeller perfomance is shown in Figure 27. The surge line is an engineering estimate of where surge occurred near recorded operating points. However, there appears to be no correlation between adiabatic efficiency and total impeller flow. This is attributed to variations in scavenge flow with respect to total impeller flow and to scatter in the temperature data. Since low pressure ratios were involved, with associated low temperature rise, a ±1°F variation in temperature results in approximately a ±2-point change in adiabatic efficiency. To obtain an indication of the effect of scavenge flow, the data were replotted with adiabatic efficiency as a function of primary flow and percentage of scavenge flow. As shown in Figure 28, a slight decrease in efficiency appears to occur with increasing scavenge flow.

The first test condition, at the design airflow of 8.0 lb/sec, was to be conducted to evaluate the characteristics of the mixed-flow impeller with a constant-area discharge flowpath. The impeller blades and discharge flowpath surfaces were heavily painted with a machinist blue paint. After obtaining performance data for the no-scavenge flow test condition, AC coarse test dust was then fed into the separator for 0.1 hr to verify the predicted location of the scavenge zone. Verification was to be obtained by a post-run inspection of where the particles produced erosion on the painted shroud. However, upon removal of the split shroud, it was found that all of the paint had been removed from the flow passage outside diameter as well as from the pressure face of the impeller blades. An area of particle concentration was also evident on the discharge passage inside diameter, as shown in Figure 29. As a result, an alternative method was employed to evaluate particle impingement on the shroud. A profilometer measurement of the shroud surface indicated that the location of maximum surface roughness agreed approximately with the predicted region of maximum particle impingement on the shroud. The scavenge zone was then machined, as previously planned, and the split shroud was reinstalled for separator tests at the specified test conditions.

29
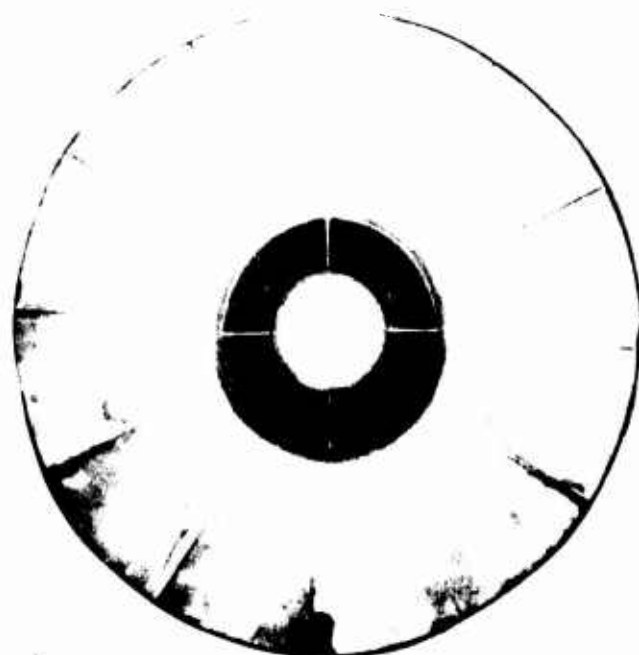
Before Straw Ingestion

After Straw Ingestion

Figure 23. Semi-Reverse-Flow Separator Inlet Before and After
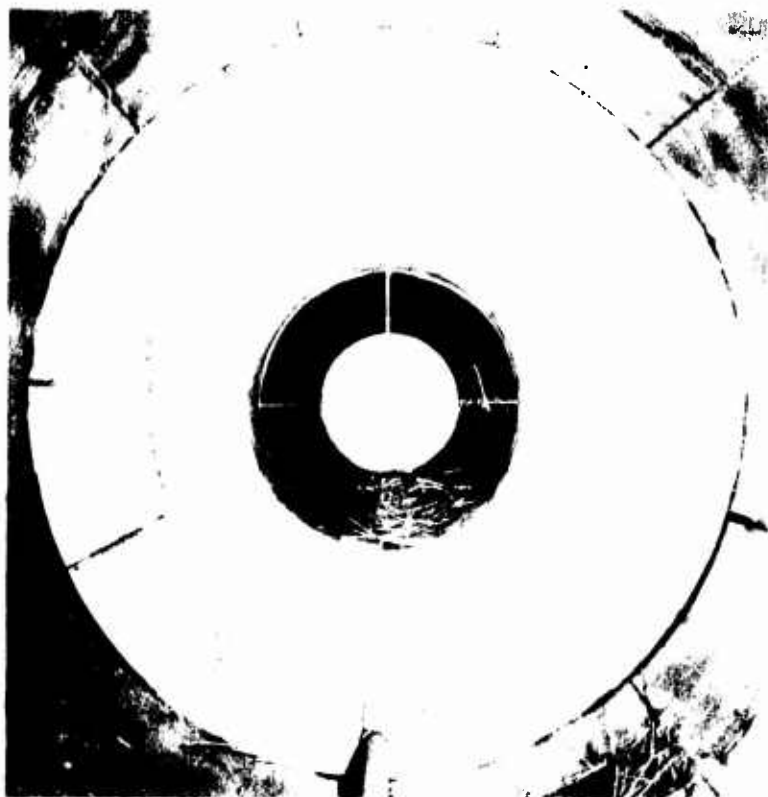Simulated Foliage-Ingestion Test.

30

Figure 24. Semi-Reverse-Flow Separator No-Swirl Configuration
Inlet After Simulated Foliage-Ingestion Test.

A maximum separation efficiency of only 58. 7% was obtained with the powered
mixed-flow separator. In Phase I of this program it was estimated that, due to
the very strong centrifugal forces acting on the particles, the powered mixed-flow
separator would demonstrate higher separation efficiency than the semi-reverse-
flow separator. However, its failure to do so may have been partially due to
random particle rebound after being struck by the high-rpm impeller blades,
which, with only one scavenge zone, could reduce particle capture. Additional
evaluation of the problem or further development of the concept was not con-
sidered to be within the scope of this program.

After completing the aerodynamic performance and separation efficiency tests,
the 20-min simulated rain-ingestion test with 1. 5 lb/sec water spray was con-
ducted at the 100%/5% test condition. There was no resultant adverse effect on
the separator; however, rotor speed decreased 300 rpm during water-spray
ingestion. The 20-min simulated foliage-ingestion test was then conducted at
the same airflow condition, using approximately 0. 8 lb of dry straw. Most of the
straw was ingested by the separator, but some straw collected on the four struts
in the inlet bellmouth and a lesser amount on the inlet guide vanes, as shown in
Figure 30. As a result, the separator airflow decreased from 8. 00 lb sec to
6. 96 lb/sec, and pressure rise decreased from 7. 13 psi to 5. 94 psi.

31

TABLE III. POWERED MIXED-FLOW SEPARATOR TEST RESULT SUMMARY

| Nominal Primary/Scavenge (% Flow)	Type of Test	Test Time (min)	Primary Airflow (lb/sec)	Scavenge Airflow (lb/sec)	Primary Airflow (% Design)	Scavenge Airflow (% Primary)	Rotor Speed (rpm)	Average Pressure Rise (psi)	Average Swirl Angle, 90 deg = axial (deg)	Average Total Temperature (°F)	Compressor Aerodynamic Efficiency (%)	Dust Separation Efficiency (%)	Actual Dust Concentration (gm/ft³)	Remarks
100%/0%	Performance	54	7.37	0.0	92.1	0.0	32,300	7.11	47.7	156	80.0			Constant-area contour performance verification.
100%/0%	Scavenge Zone Verification	6	7.37	0.0	92.1	0.0	32,300						0.0168	Scavenge zone verification test.
100%/5.0%	Performance	15	7.49	0.26	93.6	3.5	36,500	7.97	49.5	180	78.5			
100%/5.0%	Sand Ingestion	9	7.71	0.31	96.4	4.0	35,500					45.8	0.0157	Run aborted due to low thrust piston pressure.
100%/5.0%	Performance	15	7.77	0.44	97.1	5.7	35,500	7.17	50.3	167	70.7			
100%/5.0%	Sand Ingestion	45	7.76	0.41	97.0	5.3	35,500					53.9	0.0152	Repeat of above 100%/5% test.
80%/5.0%	Performance	15	6.38	0.33	79.8	5.2	25,100	3.05	53.4	117	72.3			Pressure rise low due to incorrect primary flow ejector pressure and impeller speed.
80%/5.0%	Sand Ingestion	45	6.38	0.33	79.8	5.2	25,100					50.7	0.0145	
60%/5.0%	Performance	15	4.82	0.24	60.3	5.0	19,700	2.26	54.6	108	80.3			
60%/5.0%	Sand Ingestion	45	4.64	0.23	60.5	4.8	19,700					53.85	0.0146	Valid test.
100%/2.5%	Performance	15	7.81	0.21	97.6	2.7	35,500	7.45	50.9	130	69.3			
100%/2.5%	Sand Ingestion	45	7.79	0.20	97.4	2.6	35,500					41.7	0.0151	Valid test.
100%/7.5%	Performance	15	7.56	0.64	94.5	8.5	35,500	6.76	49.8	180	68.0			
100%/7.5%	Sand Ingestion	45	7.59	0.64	94.9	8.4	35,500					58.7	0.0154	Valid test.
80%/5.0%	Performance	15	6.28	0.36	78.5	5.7	28,600	5.07	51.2	140	78.1			
80%/5.0%	Sand Ingestion	33	6.28	0.36	78.5	5.7	28,600					57.1	0.0150	Run aborted due to electrical power failure.
80%/5.0%	Sand Ingestion	45	6.19	0.36	77.4	5.8	28,600					55.9	0.0152	Repeat of above separation efficiency test.
100%/5.0%	Performance	20	7.65	0.42	95.6	5.5	35,500	7.12	50.4	165	70.0			Ingestion base performance test.
100%/5.0%	Post-Rain Performance	20	7.59	0.42	94.8	5.5	35,500	7.18	50.8	157	74.9			Post-rain ingestion performance test.
100%/5.0%	Post-Foliage Performance	20	6.60	0.36	82.5	5.5	35,500	5.94	52.4	175	54.5			Post-foliage ingestion performance test.
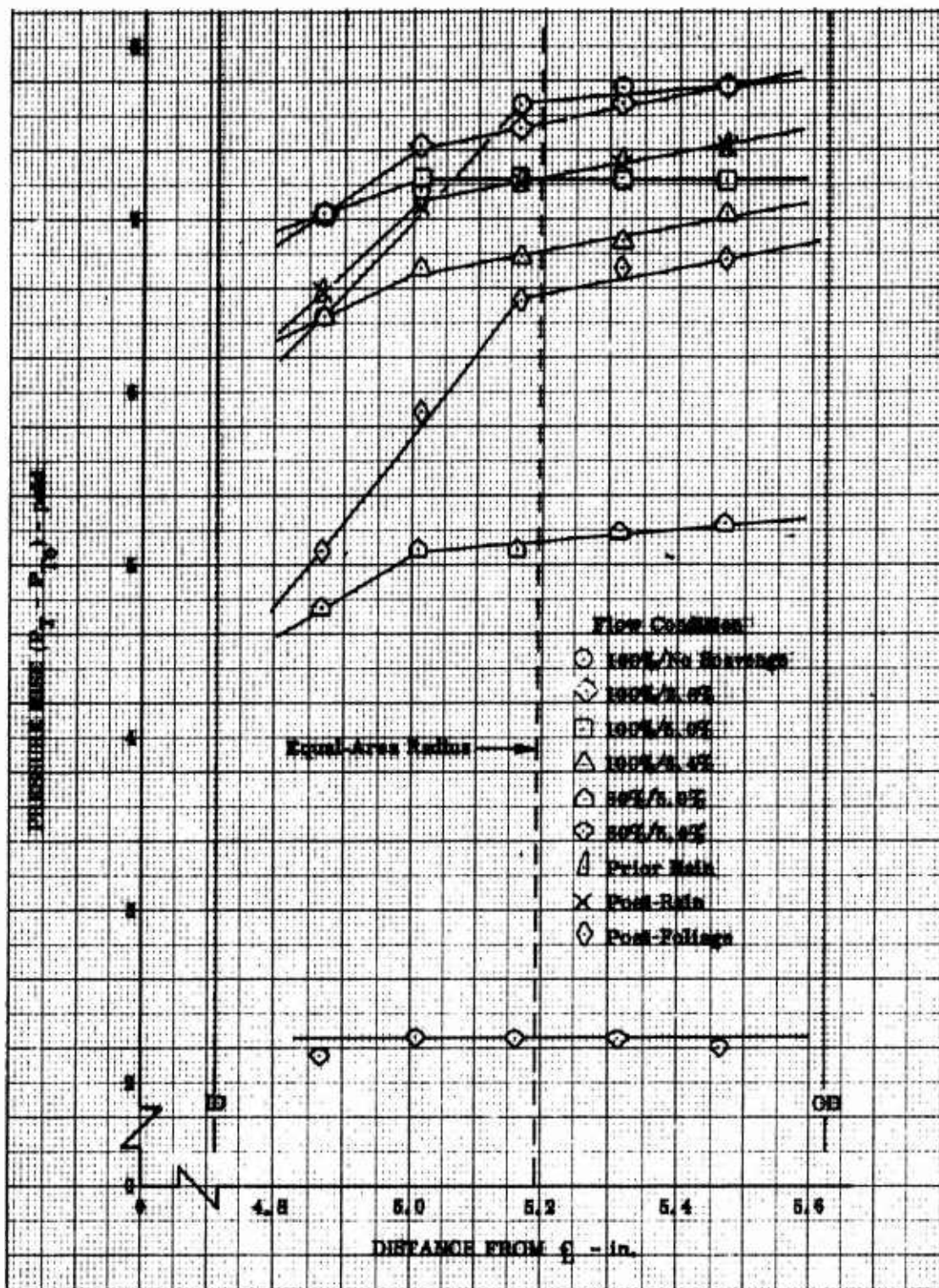
Figure 25. Powered Mixed-Flow Separator Total Pressure Rise
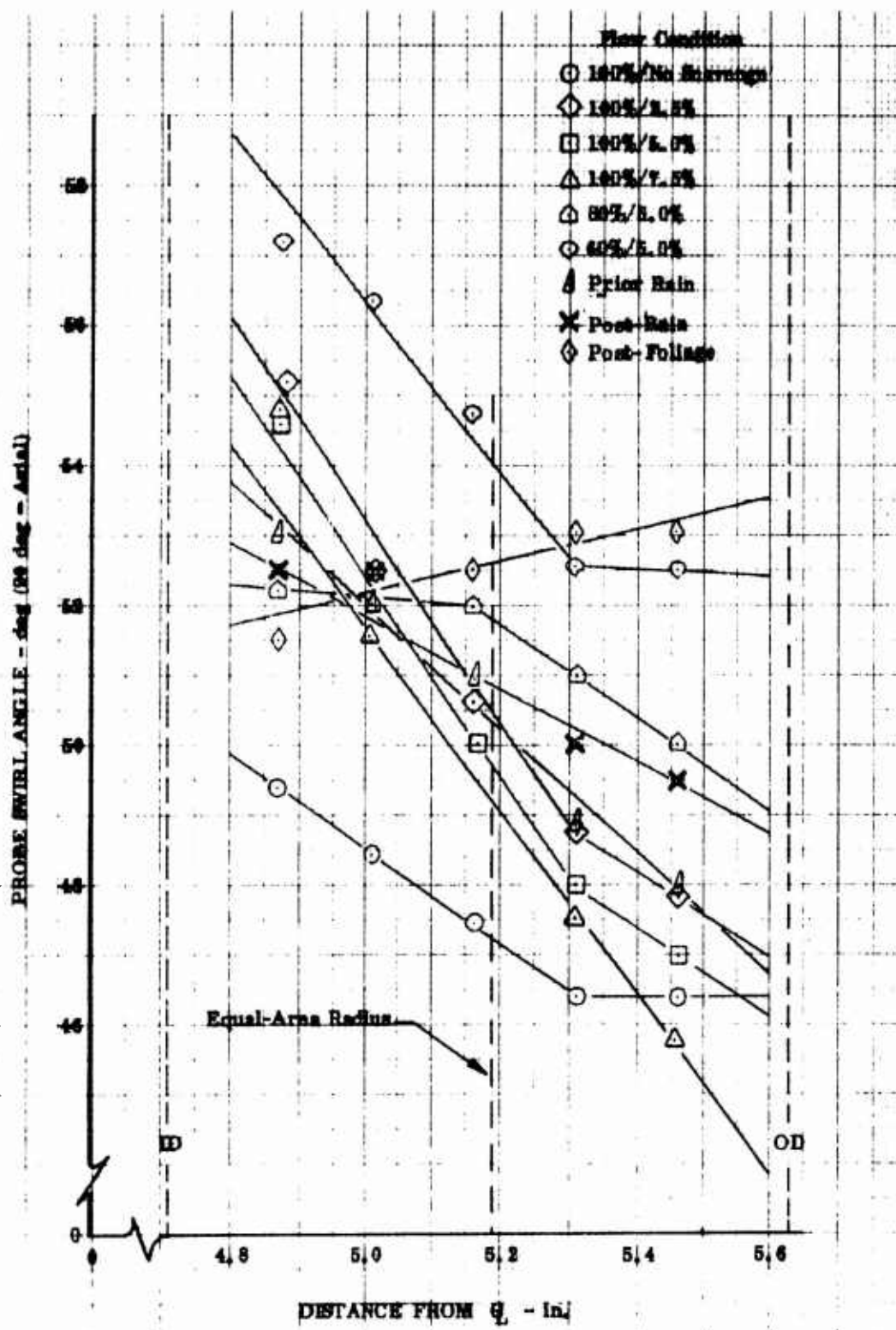Profiles at Various Test Conditions.

33

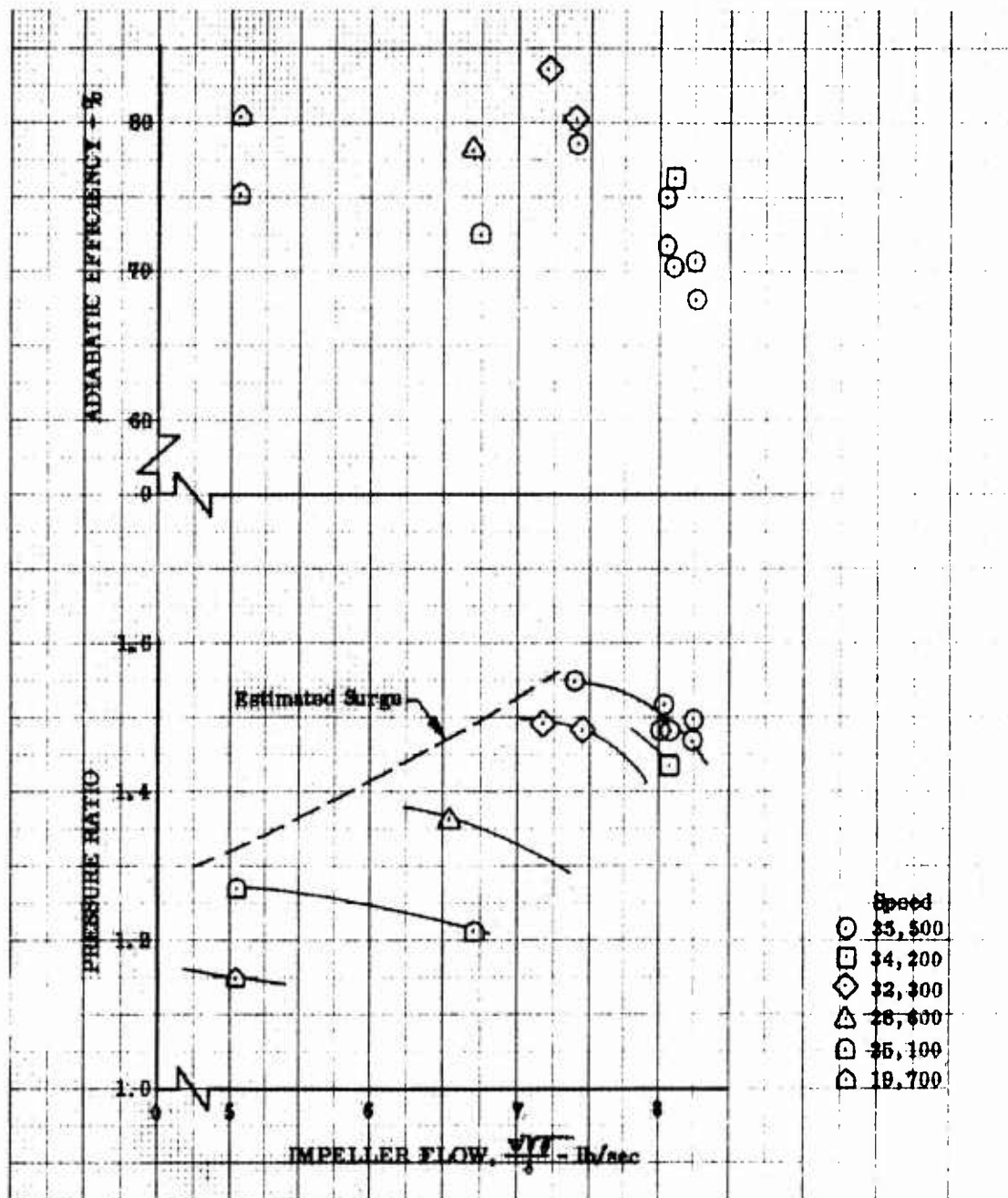Figure 26. Powered Mixed-Flow Separator Swirl Profiles at Various Test Conditions.

34

Figure 27. Mixed-Flow Impeller Aerodynamic Performance Map.

35

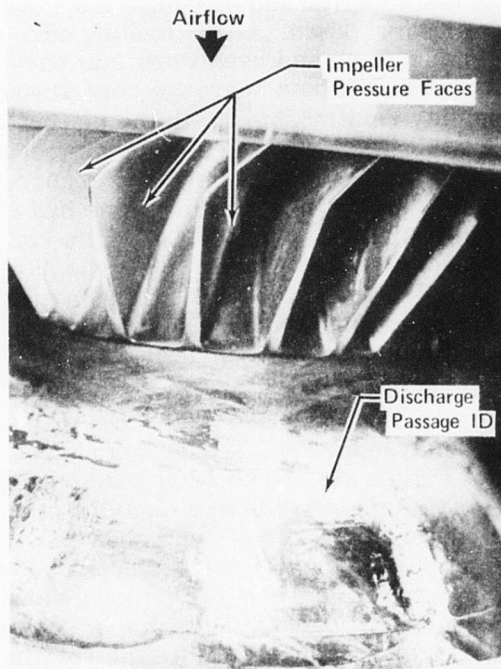Figure 29. Mixed-Flow Impeller Adiabatic Efficiency.

36

Figure 29. Impeller and Constant-Area Flow Passage After
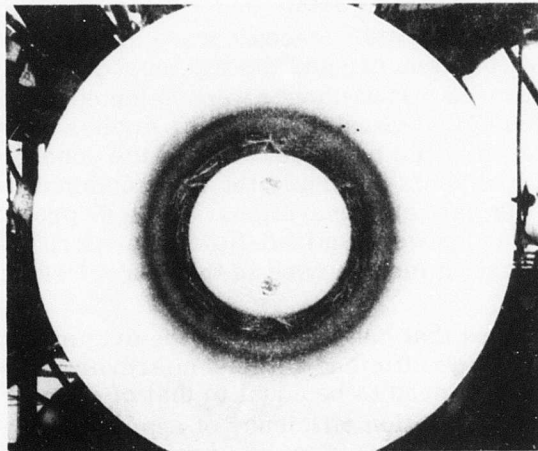0.1 Hour of Sand Ingestion.

Figure 30. Powered Mixed-Flow Separator Inlet After
Foliage-Ingestion Test.

A post-test inspection of the impeller and scavenge zone housing was made to check for visible signs of wear. The impeller leading edge showed considerable wear, except at the tip, and a notch had been worn into each impeller blade in the area where the impeller case and scavenge zone shroud meet, as shown in Figure 31. This assembly relationship, with the mating impeller case removed, is shown in Figure 32. An inspection of the stainless steel mating part revealed that the inside diameter was still within bleuprint tolerance; however, the aluminum scavenge shroud inside diameter at the interface had increased 0.040 in., thus causing a step. Figure 32 also shows that all paint had been removed from the pressure side of the impeller blades, while only the paint in the vicinity of the blade leading edge was removed from the back face. In addition, essentially all paint had been removed from the hub, indicating that in spite of the strong centrifugal forces present, particles were still contacting the hub.

Dust removed by both separators and a sample of the AC coarse dust used during the tests were wet-sieve analyzed. The distribution curves derived from the analysis are presented in Figure 33. Separation efficiency as a function of particle size was calculated using the distribution data and previously determined overall separation efficiencies. The results are shown in Figure 34. A separation efficiency in excess of 90% on particles 20 microns and larger was calculated for the semi-reverse-flow separator when swirl vanes were utilized. The calculation of a separation efficiency approaching 200% for the powered mixed-flow separator in the 20 micron size range is attributed to the rotating impeller blades fracturing the larger particles into small ones, hence creating more fine particles than were originally present in the AC coarse test dust. The separation efficiency values in 10 micron range calculated for both particle separators are probably low because it was difficult to obtain a sample from the final filter that retained all the fines, i.e., the paper elements used in the test facility filters had a tendency to retain fines which could only be removed by blowing them out with an air-hose.

In Phase I of this program, eight particle separator concepts were considered to be feasible. The eight separator concepts were evaluated with respect to each other for each of ten rating factors, and the two most promising concepts, "semi-reverse-flow" and "powered mixed-flow", were selected for feasibility demonstration. Having tested both separator concepts, further evaluation of the justification for their selection could be made. One of the concepts considered was a vortex-tube separator, which is presently the most common and efficient industrial means of engine inlet air particle separation. Table IV presents a comparison of the semi-reverse-flow and powered mixed-flow separators to a vortex-tube separator, based on the 10 rating factors used in the Phase I evaluation.

There are several changes that can be made to the original Phase I evaluations. In the category of separation efficiency, the semi-reverse-flow separator demonstrated an efficiency considered to be equal to that of current vortex-tube separators, which have an installed separation efficiency of approximately 86.5% on AC coarse test dust (Reference 2). However, since the powered mixed-flow separator demonstrated a maximum efficiency nearly 30 percentage points less than that of vortex-tube elements, it has to be judged inferior. It is felt that the semi-reverse-flow separator is only equal to vortex tubes in the category of operation in an adverse environment, due to the collecting of straw on the swirl vanes during foliage
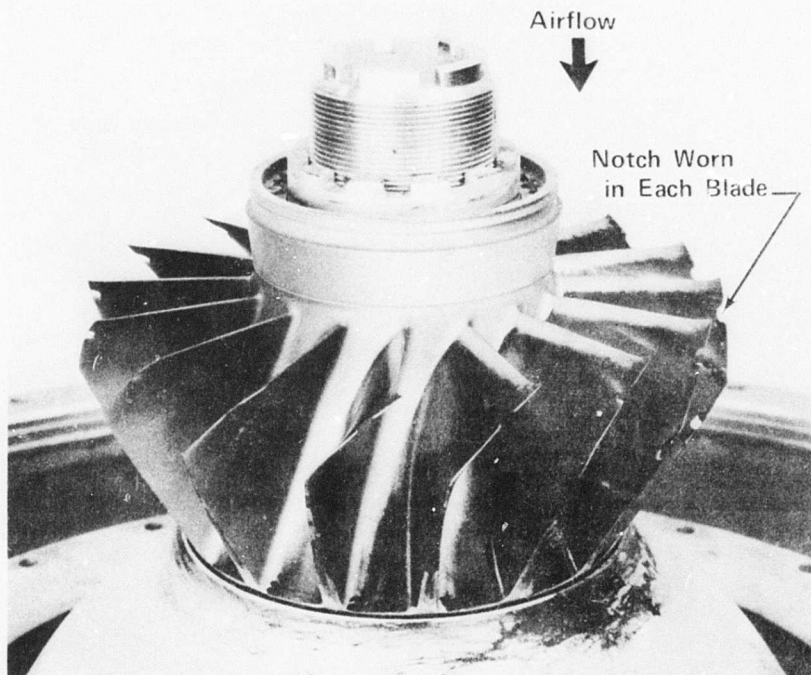
Airflow

Notch Worn
in Each Blade

Figure 31. Mixed-Flow Impeller Wear After 5.3 Hours of Sand
Ingestion.

ingestion. Also it was considered that the semi-reverse-flow separator had to
be judged equal to a vortex-tube separator in the category of self-contained oper-
ation. Since separation efficiency was found to be strongly dependent upon high
scavenge flow rates, an exhaust-gas-driven ejector system would be needed to
provide the high scavenge flows. It is estimated that from 0.5% to 1.5% power
loss would result from back-pressuring the turbine during ejector operation.

Although the semi-reverse-flow separator with swirl vanes demonstrated a
pressure drop approximately 30% less than current inlet particle separators,
some additional pressure loss would be incurred to remove the residual swirl
prior to entering the compressor inlet. However, this pressure loss penalty
would be decreased for an engine using inlet guide vanes, as they could be de-
signed to provide the required compressor pre-whirl while controlling the
residual swirl from the separator.

Anti-icing capability of the semi-reverse-flow and powered mixed-flow separators
was not evaluated, however both could readily be anti-iced by heating the struts
and vanes either electrically or with the use of compressor bleed air. No practical
means of anti-icing a conventional vortex tube separator has been demonstrated.
Determination of actual power requirements for anti-icing either separator was
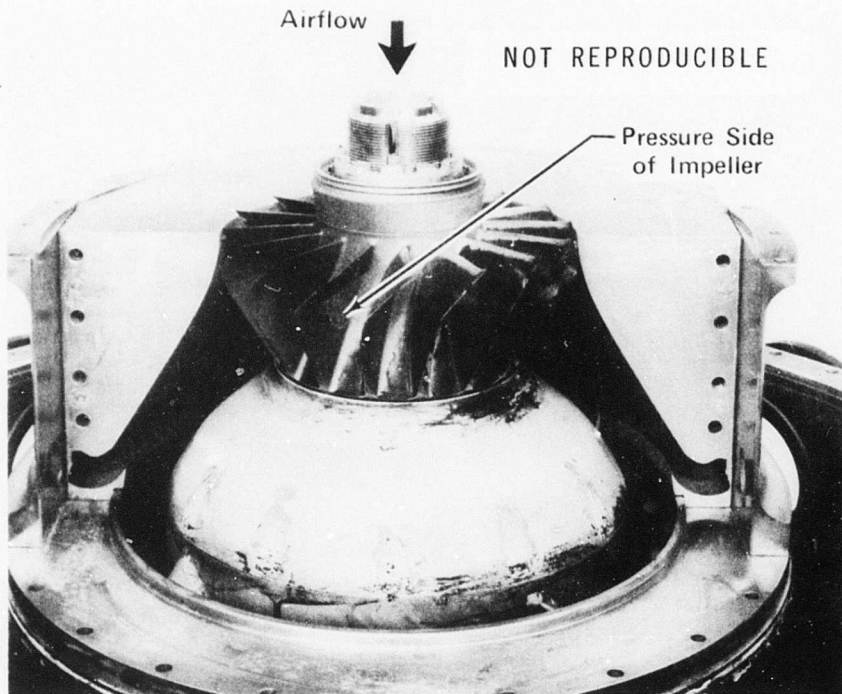not within the scope of the program.

39

Figure 32.   Post-Test View of Impeller and Scavenge-Zone
Contour Split Shroud.

Determination of localized concentration effect and a detailed weight and volume
analysis of flight-type hardware was also beyond the scope of the program. However,
it is estimated that both separators would be inferior to vortex tubes in localized
concentration effect. Dust which is not separated by the semi-reverse-flow
separator would be concentrated on the outer diameter of the compressor inlet flow
path, thus entering the compressor inlet in the region of the compressor blade
tip's. Dust passing through the powered mixed-flow separator is subjected to a
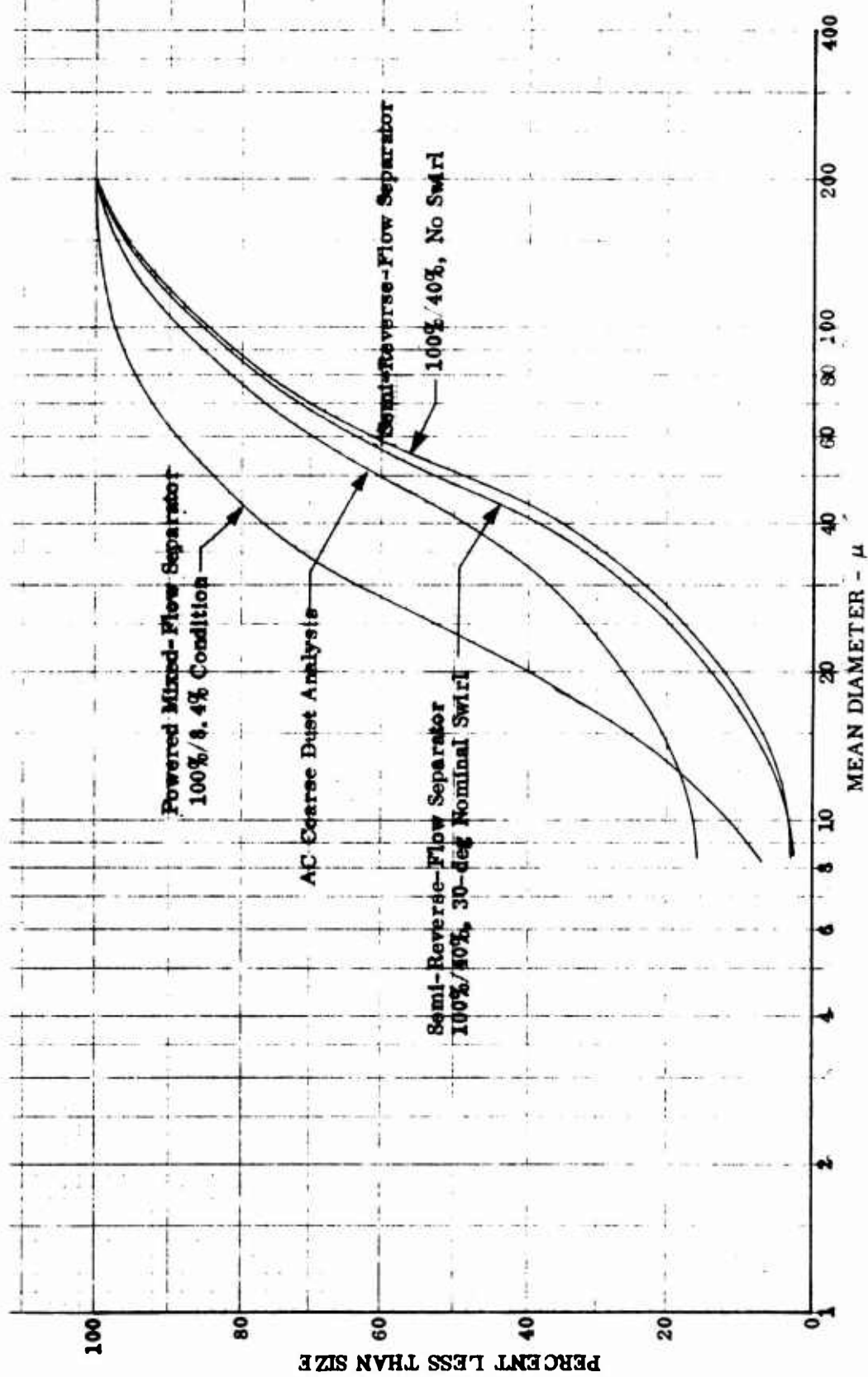strong centrifugal field, which concentrates dust at the impeller blade tips.

Figure 33. Wet-Sieve Analysis of Filtered Test Dust From Separator Test Program.
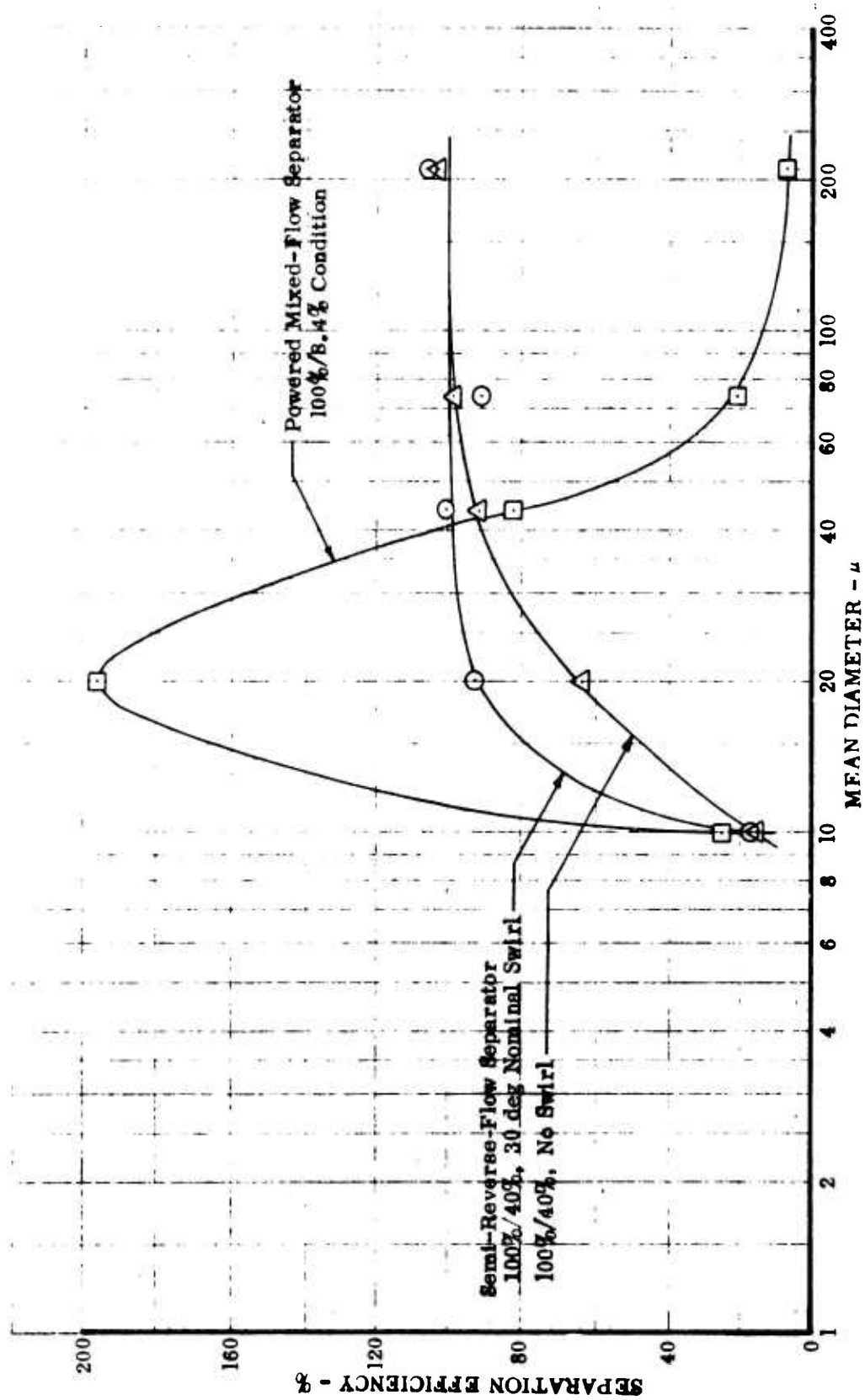
41

Figure 34. Calculated Separation Efficiency Versus Particle Size.

42

Rating Factors	Phase I Evaluation			Post-Test Evaluation		
	Inferior	Equal	Superior	Inferior	Equal	Superior
Separation Efficiency	S	P		P	S	
Effect on Engine Performance			S, P			S, P
Operation In Adverse Environment			S, P		S	P
Reliability	P	S		P		S
Weight			S, P			S, P
Volume			S, P			S, P
Maintainability	P	S		P		S
Cost			S, P			S, P
Localized Concentration Effect	S, P			S, P		
Self-Contained Operation			S, P		S	P

Key: S – Semi-Reverse-Flow
P – Powered Mixed-Flow

TABLE IV. COMPARISON OF SEMI-REVERSE-FLOW AND POWERED MIXED-FLOW SEPARATORS TO VORTEX TUBES

TASK 3 - RETEST OF SEMI-REVERSE-FLOW SEPARATOR

When operation of the semi-reverse-flow separator in an adverse environment was simulated with a foliage-ingestion test, grass and straw collected on the leading edges of the swirl vanes and greatly increased the pressure drop through the separator as shown by Figure 23. A new swirl vane was designed to permit passage of most of the foliage through the separator. The new swirl vane is of identical contour to the original vane, except that it has a sloped leading edge and reduced height to permit foliage to pass between the vane tips and the outer case. The new foliage ingestion swirl-vane configuration is shown in Figure 35, and Figure 36 compares the original swirl-vane assembly to the new foliage ingestion swirl-vane assembly. Swirl-vane number was increased from 18 to 24 to compensate partially for the reduced surface area available for swirling the particles.

Testing the new swirl-vane configuration was conducted as described previously for the semi-reverse-flow separator, using identical test-stand setups and testing procedures. Separator efficiency at the design airflow condition of 8.0 lb/sec and 40% scavenge flow was determined to be 88.9%, with an average total pressure drop of 6.0 in. H_2O. A plot of total pressure profiles obtained by traversing the flowpath downstream of the separator is shown in Figure 37. The original pressure profile is also shown for reference. The slopes of the modified swirl-vane pressure profiles are reversed from the original design data, suggesting that aerodynamic separation was occurring off the tips of the unshrouded vanes. Swirl-angle profiles were also determined downstream of the separator and are shown in Figure 38. They are similar to the original profile, which is also shown for reference. The foliage ingestion test was conducted, as previously described, using 1.1 lb of dry straw, also at the design condition of 100%/40% airflow. The reduced height of the modified swirl vanes permitted most of the straw to pass through the separator, except for a lump that became lodged in one quarter of the inlet, as shown in Figure 39. This increased the pressure drop to approximately 10 in. H_2O and changed the pressure profile, as indicated in Figure 37. A test was made to evaluate the capability of separating small nuts, bolts, and washers introduced into the separator inlet also at the 100%/40% airflow condition. The FOD ingestion items (small nuts, bolts, washers and Dzus fasteners) are shown in Figure 40. A test was also included that simulated an engine start with potential FOD items resting in the bellmouth inlet. In both tests, all FOD items were separated from the primary airflow (i.e., 100% separation efficiency).
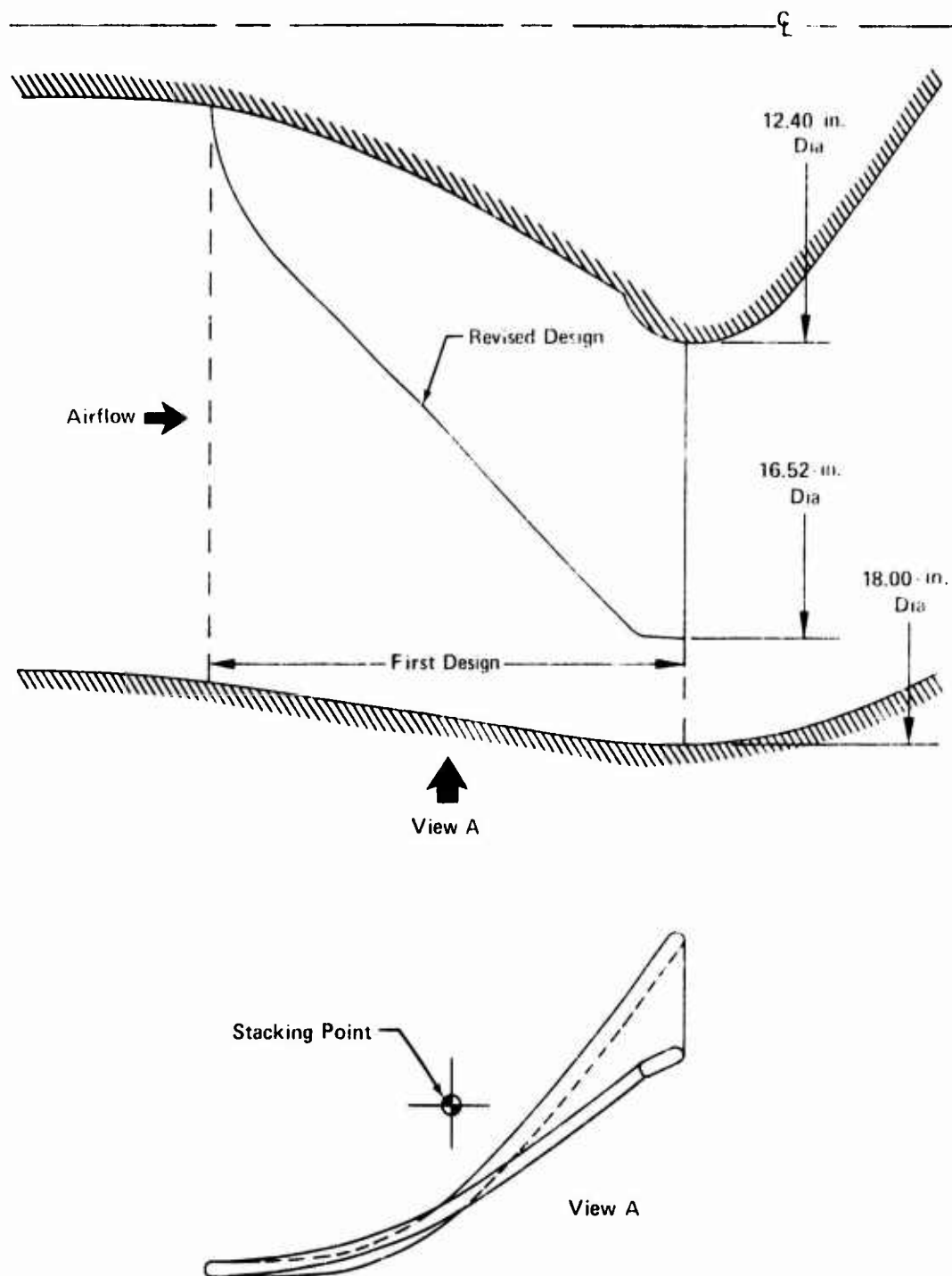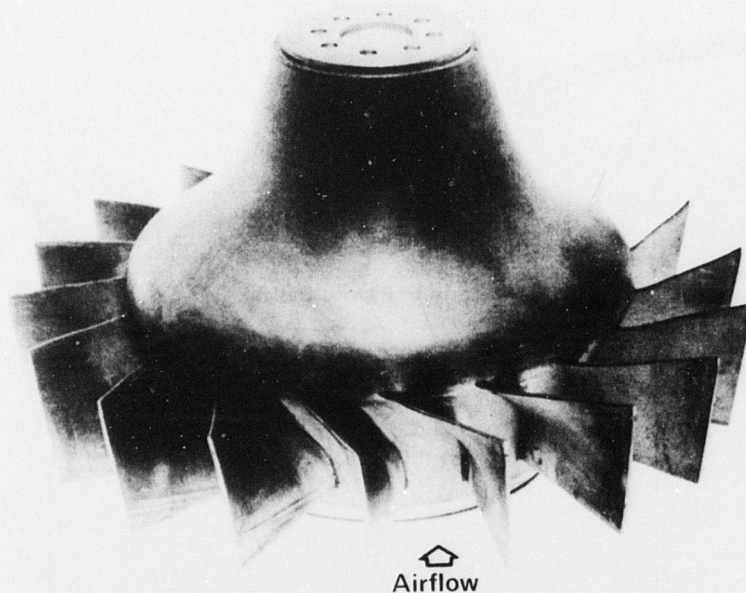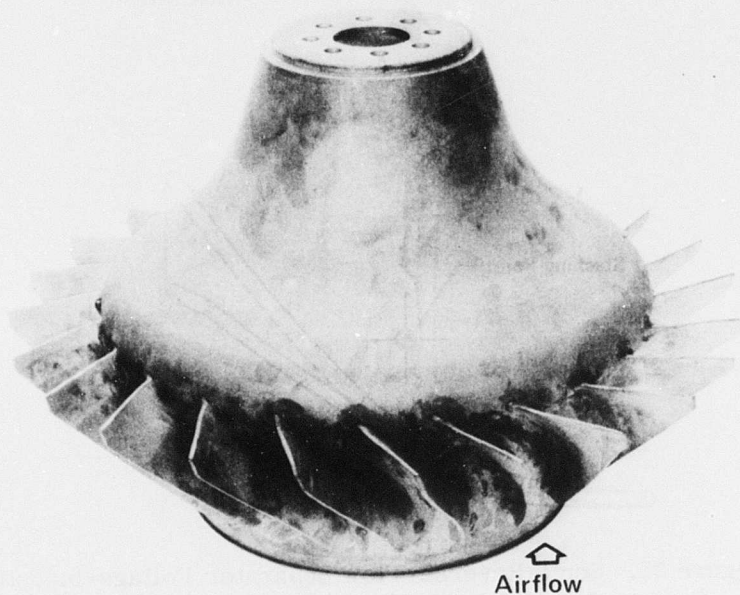
Figure 35. Semi-Reverse-Flow Separator Foliage-Ingestion Swirl-Vane Configuration.

⇧
Airflow

Original Swirl-Vane Configuration

⇧
Airflow

Swirl Vanes Modified To Improve
Foliage Ingestion Capability

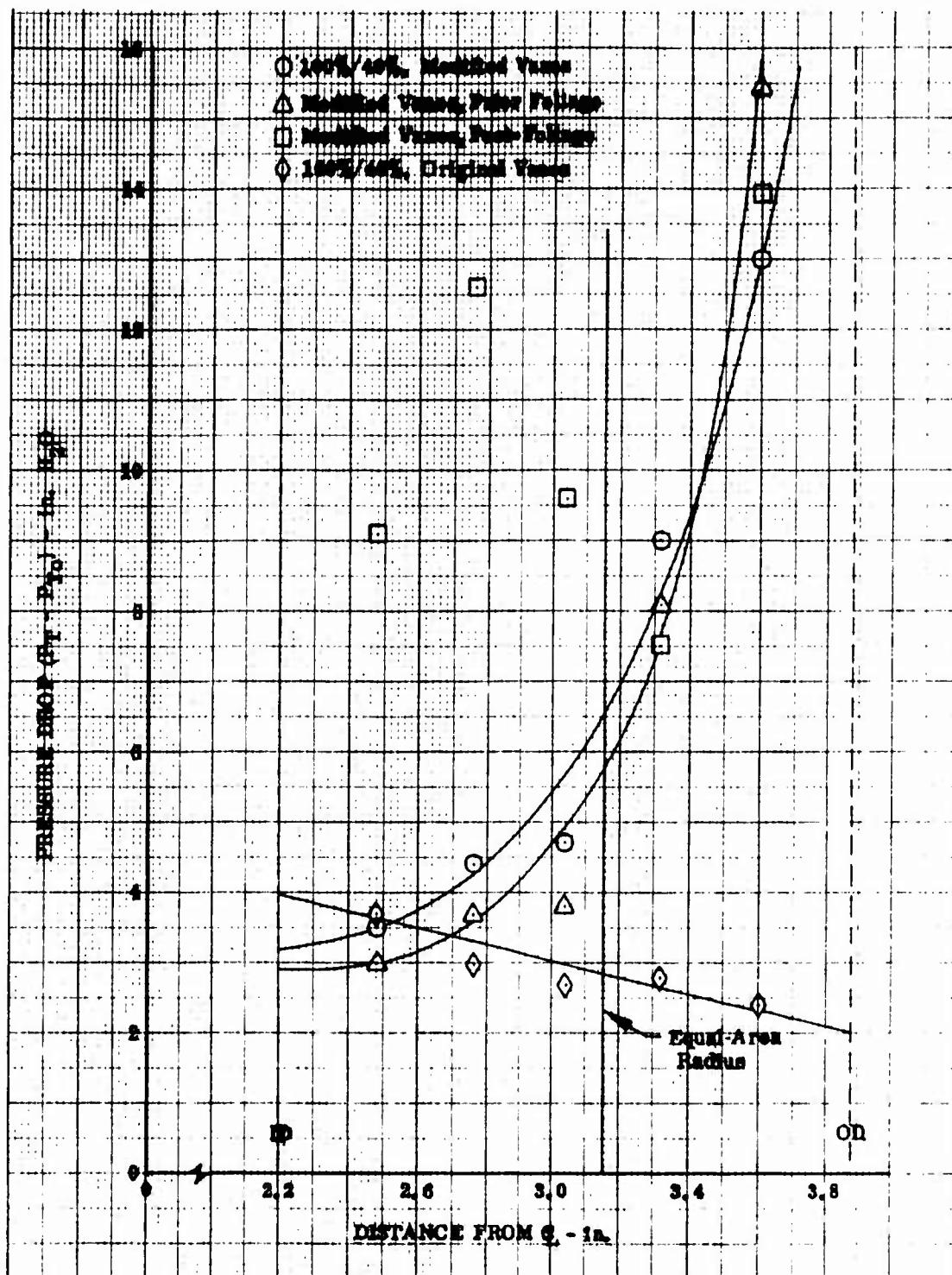Figure 36. Comparison of Semi-Reverse-Flow Separator
Swirl Vanes.

46

Figure 37. Total-Pressure-Drop Profiles From Foliage-Ingestion Swirl-Vane Tests.
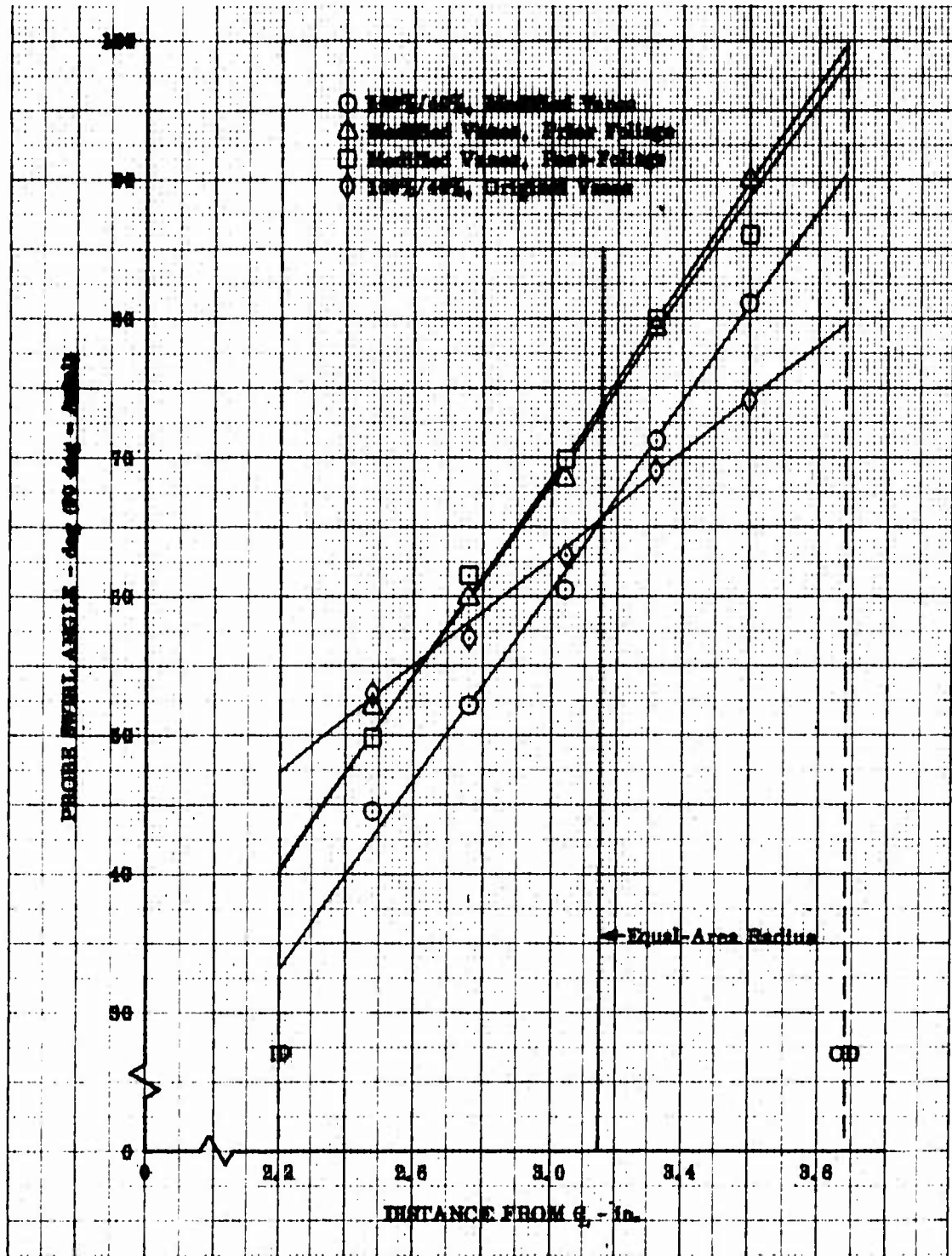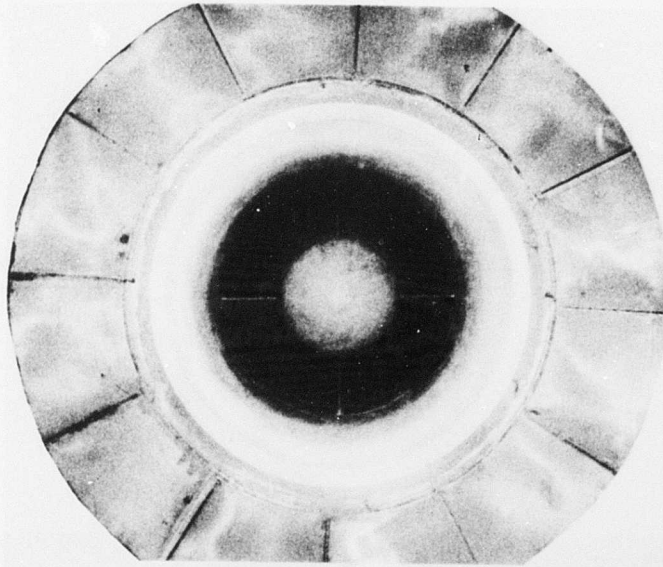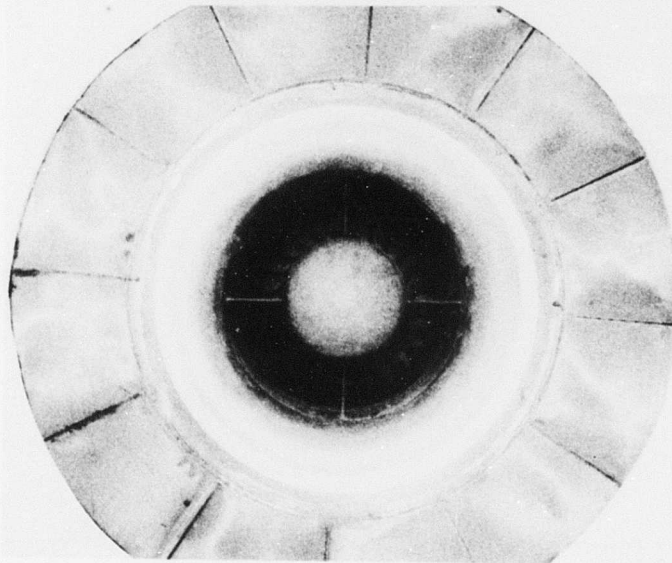
47

Figure 38. Swirl Profiles From Foliage-Ingestion Swirl-Vane
Tests.

48

Before Straw Ingestion

After Straw Ingestion

Figure 39. Foliage-Ingestion Swirl Vanes Before and After
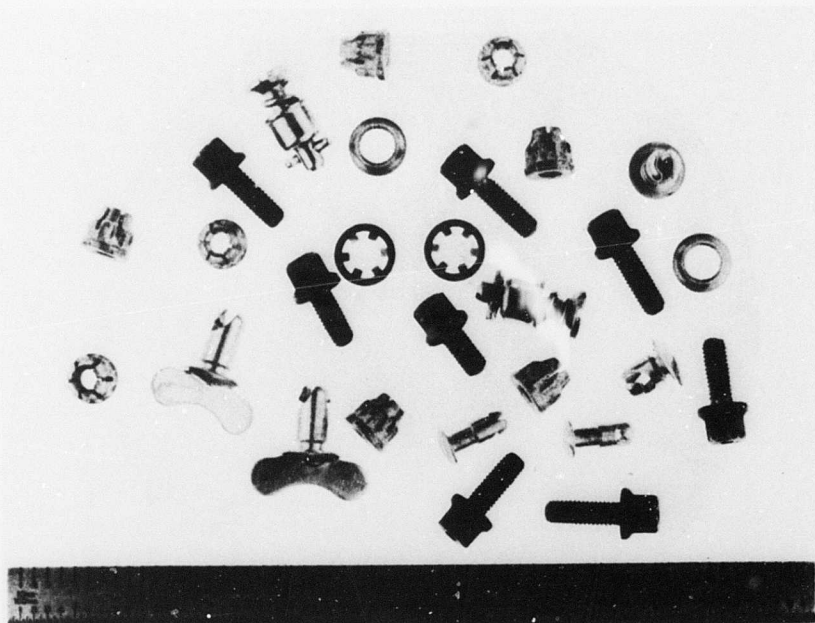Simulated Foliage-Ingestion Test.

49

Figure 40. FOD Ingestion Items.

50

CONCLUSIONS

1. At design airflow of 8 lb/sec and 40% scavenge flow, the semi-reverse-flow separator demonstrated 88.5% separation efficiency on AC coarse test dust with an average pressure drop of 2.8 inches H_2O.

2. At design airflow of 8 lb/sec, the powered mixed-flow separator demonstrated a maximum separation efficiency on AC coarse test dust of 58.7% with 8.4% scavenge flow and an average pressure rise of 6.76 psi.

3. In Phase I of the program the semi-reverse-flow and powered mixed-flow separators were evaluated with respect to other separator concepts and both were considered to be potentially superior to current separator designs. Based on the Phase II results, the semi-reverse-flow separator is feasible as an integral part of an engine inlet, and the design is considered to be superior to current engine air particle separators for the majority of the aspects investigated.

4. The powered mixed-flow separator is feasible; however, it is inferior to current engine air particle separators. Additional development might significantly improve separation efficiency, but impeller wear would still be a problem.

5. Neither the semi-reverse-flow separator nor the powered-mixed-flow separator should be considered an optimum design. A suitable scavenge system, e.g., engine exhaust-gas ejector, has not been demonstrated for the semi-reverse-flow concept.

LITERATURE CITED

1. McAnally, III, Wm. J., and Max T. Schilling, INVESTIGATION OF FEASIBILITY OF INTEGRAL GAS TURBINE ENGINE SOLID PARTICLE INLET SEPARATORS, PHASE I, FEASIBILITY STUDY AND DESIGN, Pratt & Whitney; USAAVLABS Technical Report 70-44, U. S. Army Aviation Materiel Laboratories, Fort Eustis, Va., August 1970, AD875953.

2. Mund, M. G., and H. Guhne, GAS TURBINES-DUST-AIR CLEANERS: EXPERIENCE AND TRENDS, American Society of Mechanical Engineers, Paper No. 70-GT-104, May 1970.